

Synthesis, biological evaluation, and molecular modeling of nitrile-containing compounds: Exploring multiple activities as anti-Alzheimer agents

Daniel Silva,¹ Eduarda Mendes,¹ Eleanor J. Summers,² Ana Neca,¹ Ana C. Jacinto,¹ Telma Reis,¹ Paula Agostinho,³ Irene Bolea,⁴ M. Luisa Jimeno,⁵ M. Luisa Mateus,¹ Ana M. F. Oliveira-Campos,⁶ Mercedes Unzeta,⁴ José Marco-Contelles,⁷ Magdalena Majekova,⁸ Rona R. Ramsay,² M. Carmo Carreiras¹

¹Research Institute for Medicines (iMed.U LISBOA), Faculty of Pharmacy, Universidade de Lisboa, Av. Professor Gama Pinto, 1649-003 Lisbon, Portugal.

²Biomedical Sciences Research Complex, University of St. Andrews, Biomolecular Sciences Building, North Haugh, St. Andrews, KY16 9ST, UK.

³Faculty of Medicine & Center for Neuroscience and Cell Biology, University of Coimbra, 30054-504 Coimbra, Portugal.

⁴Institut de Neurociències i Departament de Bioquímica i Biologia Molecular, Facultat de Medicina, Universitat Autònoma de Barcelona (UAB), Bellaterra (Barcelona), Spain.

⁵Centro de Química Orgánica “Lora Tamayo” (CSIC), C/ Juan de la Cierva 3, 28006 Madrid, Spain.

⁶Centro de Química, Universidade do Minho, Campus de Gualtar, PT-4710-057 Braga, Portugal.

⁷Laboratory of Medicinal Chemistry, Institute of Organic Chemistry (CSIC), Madrid, Spain.

⁸Center of Experimental Medicine, Institute of Experimental Pharmacology and Toxicology, Slovak Academy of Sciences, Dubravska cesta 9, 84104 Bratislava, Slovakia.

Correspondence

M. Carmo Carreiras

e-mail: micarreiras@gmail.com

e-mail: mcdamaso@ff.ulisboa.pt

Rona Ramsay

e-mail: rrr@st-andrews.ac.uk

Acknowledgments

This collaborative work was enabled by COST Action CM1103, *Structure-based drug design for diagnosis and treatment of neurological diseases*.

We thank our funding sources: COST Actions D34 and CM1103 for Short-term Scientific Mission funding (EM, DS, MM); the School of Biology at the University of St. Andrews (EJS, RRR); the Research Institute for Medicines (iMed.U LISBOA), Faculty of Pharmacy, Universidade de Lisboa (AN, ACJ, TR, MCC); FCT, the Portuguese Foundation for Science and Technology (Project PTDC/SAU-NEU/64151/2006 (MCC), and project grant (DS) Vega 2/0127/18 and the contract No. APVV-15-0455 of Slovak Research and Development Agency (MM).

Abstract

Based on the MAO inhibition properties of aminoheterocycles with a carbonitrile group we have carried out a systematic exploration to discover new classes of carbonitriles endowed with dual MAO and AChE inhibitory activities, and A β anti-aggregating properties. Eighty-three nitrile-containing compounds, 13 of which are new, were synthesized and evaluated. *In vitro* screening revealed that **31**, a new compound, presented the best lead for trifunctional inhibition against MAO A (0.34 μ M), MAO B (0.26 μ M) and AChE (52 μ M), while **32** exhibited a lead for selective MAO A (0.12 μ M) inhibition coupled to AChE (48 μ M) inhibition. Computational analysis revealed that the malonitrile group can find an advantageous position with the aromatic cleft and FAD of MAO A or MAO B. However, the total binding energy can be handicapped by an internal penalty caused by twisting of the ligand molecule and subsequent disruption of the conjugation (**32** in MAO B compared to the conjugated **31**). Conjugation is also important for AChE as well as the hydrophilic character of malonitrile that allows this group to be in close contact with the aqueous environment as seen for **83**. Although the effect of **31** and **32** against A β ₁₋₄₂, was very weak, the effect of **63** and **65**, and of the new compound **75**, indicated that these compounds were able to disaggregate A β ₁₋₄₂ fibrils. The most effective was **63**, a (phenylhydrazinylidene)propanedinitrile derivative that also inhibited MAO A (1.65 μ M), making it a potential lead for Alzheimer's disease application.

KEYWORDS:

nitrile-containing compounds,
Alzheimer's disease,
MAO inhibitors,
AChE inhibitors,
A β ₁₋₄₂ disaggregating agents,
in silico study

1 INTRODUCTION

Alzheimer's disease (AD), the most common neurodegenerative disease, is marked by progressive decline in a variety of higher cortical functions. AD patients share common clinical and neuropathological features, notably intracellular neurofibrillary tangles and extracellular senile plaques, the two major pathological hallmarks (Korabecny et al., 2018). Neurofibrillary tangles are formed by hyperphosphorylated tau protein, while senile plaques are aggregates of amyloid β ($A\beta$) peptides associated with several proteins, metal ions, and enlarged axons and synaptic terminals. Moreover, reduced levels of acetylcholine (ACh) in specific brain regions that mediate memory and learning functions, loss of neurons and synapses, high levels of metal ions like Cu^{2+} , Zn^{2+} , Fe^{3+} , mitochondrial dysfunction, inflammation and the associated oxidative stress (OS) represent features of this multifactorial disease (Das & Basu, 2017; Jakob-Roetne & Jacobsen, 1992). Acetylcholinesterase (AChE) hydrolyzes extracellular ACh into choline and acetic acid, thus preventing the overstimulation of nerve cells. However, in AD, loss of cholinergic neurons means that stimulation of nerve cells by ACh is reduced, and neuronal communication is hindered. AChE inhibitors improve neuronal communication by preventing the breakdown of ACh (Das & Basu, 2017).

Noncatalytic functions of AChE have been suggested in multiple physiological processes, such as cell adhesion, neurite growth, apoptosis, and $A\beta$ aggregation (Wang & Zhang, 2019). AChE interacts with $A\beta$ by the hydrophobic environment close to the peripheral anionic site (PAS) (Johnson & Moore, 1999; Inestrosa et al., 1996; De Ferrari et al., 2001), forming stable AChE- $A\beta$ complexes, (Alvarez et al., 1997; Alvarez et al., 1998) and causing an increase in the neurotoxicity of the $A\beta$ fibrils (Muñoz & Inestrosa, 1999; Reyes et al., 2004). In addition, AChE activities have also been reported to correlate with the density of $A\beta$ deposition in the AD brain (Arendt et al., 1992). Recent experiments suggest that during the early stage of AD, $A\beta$ enters the mitochondria increasing the generation of free radicals and might induce OS. $A\beta$ and amyloid precursor protein (APP) were also reported in the mitochondrial membranes of post-mortem brain and found to be responsible for disruption of electron transport chain to cause irreversible neurodegeneration and cell damage (Sharma et al., 2019).

Monoamine oxidase (MAO) is the major metabolic enzyme responsible for the deactivation of the monoamine neurotransmitters generating the corresponding aldehyde, ammonia, and hydrogen peroxide as metabolic products (Ramsay, 2016). Since MAO catalytic activity produces hydrogen peroxide, the increase in MAO B activity in AD and Parkinson's disease (PD) brain tissues is considered to contribute to the initiation of OS and the consequent deleterious effects to the cell. Thus, in addition to their ability to elevate the levels of monoamines in the brains of AD patients, both MAO A and B inhibitors may prevent OS by decreasing the formation of reactive oxygen species (Ramsay, 2016; Ramsay & Tipton, 2017). MAO B expression is generally elevated in AD (Kennedy et al., 2003), decreasing monoamine levels. Some work proposes that MAO B is also suggested to associate with β -secretase, γ -secretase and to regulate neuronal $A\beta$ peptide levels (Hroudova et al., 2016; Schedin-Weiss et al., 2017). Elevated MAO could be also associated with the formation of neurofibrillary tangles (Hroudova et al., 2016). MAO A also influences monoamine levels, particularly serotonin in depression, (Bortolato & Shih, 2011). MAO A levels, regulated by genetic and environmental factors, including stress, hormonal deregulation and food influences, are up or down or unchanged in various brain areas (Naoi et al., 2018). Recent evidence suggests that MAO-A generated ROS is involved in quality control signaling in mitochondria (Ugun-Klusek et al., 2019; <https://doi.org/10.1016/j.redox.2018.10.003>).

However, the role of MAO A in the trafficking and the health (and hence energy output) of mitochondria is still poorly understood. In AD patients, MAO A level changes seem to involve multiple mechanisms influencing cell survival (Cai, 2014). Due to the multifactorial nature of AD, design strategies have been envisaged for the development of different series of multifunctional drugs. In addition to MAO inhibition, multitarget-directed ligand (MTDL) properties can include brain permeable iron chelation, ChEs inhibition, anti-A β aggregation, and neuroprotection among other properties (Unzeta et al., 2016).

Previous studies have indicated that the MAO inhibitory activity of several compounds is potentiated by cyanide (Davison, 1957; Ramadan et al., 2007). The potentiating effect of cyanide can be ascribed to an activation mechanism whereby cyanide assists the binding of the inhibitor to the enzyme (Davison, 1957; Juárez-Jiménez et al., 2014). A series of carbonitrile-containing aminoheterocycles were examined experimentally and computationally to explore the role of nitriles in determining the inhibitory activity against MAO. Dicarbonitrile aminofurans were found to be potent, selective inhibitors against MAO A (Juárez-Jiménez et al., 2014). An earlier study examined the inhibition of MAO B by a series of C4-substituted phthalonitriles and a series of homologs lacking the nitrile units (Manley-King et al., 2012). It was found that the nitrile unit was a prerequisite for high binding affinity to both MAO A and MAO B. The high binding affinities to MAO B were ascribed to the highly polar nature of the nitrile group. Modeling studies indicated that the nitrile group interacts with the polar regions in the substrate cavity of the MAO B enzyme (Manley-King et al., 2012; Van der Walt et al., 2012; Chirkova et al., 2015). The carbonitrile function has also been introduced by other research groups in compounds either with the ChEs inhibitory activity (Samadi et al., 2010; Samadi et al., 2011; Samadi et al., 2012; Samadi et al., 2013) or dual ChEs and MAO inhibitory activities (Samadi, Chioua, Bolea et al., 2011).

Since the nitrile group may raise concerns regarding cyanide release, published information on diverse nitrile-containing drugs, research compounds, and *in vivo* metabolism of carbonitrile derivatives was closely examined. Structurally diverse nitrile-containing pharmaceuticals are prescribed for a variety of medical treatments, for example the selective serotonin re-uptake inhibitor and antidepressant drug citalopram, the non-purine xanthine oxidase inhibitor for the treatment of hyperuricemia febuxostat, the aromatase inhibitor and anticancer agent letrozole, and the non-nucleoside reverse transcriptase inhibitors and anti-HIV drug etravirine (Fleming et al., 2010; Jones et al., 2010). Regarding letrozole and etravirine, both exhibit two nitrile units as does the analog of etravirine, rilpivirine (Reznicek et al., 2017). In drug design, aromatic chloride is very often replaced by an aromatic nitrile since this exchange can impart desirable properties to the resulting molecule particularly when the potency is similar, or even improved. Thus, the lipophilicity of the molecule will be significantly reduced along with enhanced metabolic stability, higher aqueous solubility and reduced toxicological outcomes (Jones et al., 2010). Due to its small size, metabolic stability and ability to act as a hydrogen bond acceptor, the nitrile functional group has been incorporated into several pharmaceutical agents (Lindsay-Scott & Gallagher, 2017). A quantitative assay involving the reaction of nitriles with glutathione and cysteine has been used as a simple *in vitro* screen to assess potential toxicity risk of candidate compounds in drug discovery and decide whether to progress with compounds in the absence of radiolabeling studies (MacFaul et al., 2009).

Regarding metabolic stability, the nitrile group is not particularly electrophilic towards free nucleophiles, even glutathione (Fleming et al., 2010; MacFaul et al., 2009) and is metabolically quite robust (Boyd et al., 2009) unless activated by adjacent electron-

withdrawing elements (Oballa et al., 2007). Odanacatib, a selective inhibitor of cathepsin K, exhibited excellent metabolic stability in hepatocyte incubations across several species. In standard incubations (2×10^6 cells/mL, 20 μ M, 2 h), a 96% recovery of the parent compound was found in rat hepatocytes and a 98% recovery was obtained in rhesus monkey hepatocytes. High recovery (>99%) was observed in both dog and human hepatocyte incubations (Gauthier et al., 2008). In most nitrile-containing drugs, the nitrile group passes through the body metabolically unaffected. Cimetidine, an H_2 receptor antagonist, after both oral and intravenous doses in man, is oxidized to the sulfoxide (6-10%) and hydroxymethyl (4%) metabolites and conjugated to the N-glucuronide (24%), presenting unchanged drug (60-70%) (Strong & Spino, 1987). The biotransformation of entacapone, a catechol O-methyltransferase inhibitor was studied in experimental animals and man by identifying their O-glucuronides in urine and plasma; in rats and dogs, O-sulfates were also abundant (Wikberg & Vuorela, 1994). Early studies with radiolabelled cromakalim, an antihypertensive agent, showed the major urinary metabolites had unchanged nitrile groups (Kudoh, 1990; Kudoh et al., 1990). Lersivirine, a non-nucleoside reverse transcriptase inhibitor, is predominantly cleared by glucuronidation and cytochrome P450-mediated oxidation whereas hydrolysis of one of the nitrile moieties to form an amide represented less than 8% of the total in plasma (Vourvahis et al., 2010). The major urinary and plasma metabolites of verapamil, a phenethylamine vasodilator, were the N-dealkylated products which retain the α -isopropylphenylacetonitrile portion of the molecule (McIlhenny, 1971).

Release of cyanide from aromatic or fully substituted carbons is not observed (Fleming et al., 2010). Rabbits converted 2,6-dichlorobenzonitrile to an extent of approximately 2% and 23% into 2,6-dichloro-4-hydroxybenzonitrile and 2,6-dichloro-3-hydroxybenzonitrile, respectively. The hydrolysis of the nitrile group appears to occur to a very minor extent. Only insignificant amounts of the amide (<0.01%) and benzoic acid (<0.001%) derivatives were found. This was supported by the observation that rabbits did not convert 2,6-dichlorobenzamide into the corresponding acid (Wit & van Genderen, 1966). However, saturated and β,γ -unsaturated aliphatic nitriles are hydroxylated in the liver at the α -carbon to form cyanohydrins with subsequent cyanide release (Hideji & Kazuo, 1984, 1986). Mandelonitrile, an agent formerly used for the treatment of urinary tract infections, bears a H atom and OH group at the α -carbon. The cyanide plus thiocyanate excreted by Wistar rats represented 86% of the dose, hippuric acid corresponded to 71%, while 13% correlated to mandelic acid (Singh et al., 1985). Epoxidation of alkenenitriles and ring opening can potentially liberate cyanide, but epoxidation is synthetically difficult (Pryde et al., 1996; Aiai et al., 1995; Miyashita et al., 1987) and metabolism at other sites appears more likely to occur (Fleming et al., 2010).

Based on the MAO inhibition properties of aminofurans with the carbonitrile group (Juárez-Jimenez J. et al., 2014), the present study aimed to identify classes of nitrile-containing compounds endowed with dual AChE and MAO inhibitory activities, and $A\beta$ anti-aggregating properties. In this context, we have carried out the synthesis, biological evaluation, and molecular modeling of a number of arylidenepropanedinitriles [compounds **16-41**, Scheme 1, Tables 1, 7, and Tables S₁, S₃, S₈, and S₉ (**Supporting Information**)], [(phenylamino)methylidene]propanedinitriles [compounds **42-52**, Scheme 2, Table 2 and Table S₆ (**Supporting Information**)], 4-amino-1-phenyl-1*H*-pyrrole-3-carbonitriles [compounds **53-57**, Scheme 3, Table 3, and Tables S₇, and S₁₀ (**Supporting Information**)], and 3-amino-1-phenyl-1*H*-pyrrole-2,4-dicarbonitriles [compounds **58-62**, Scheme 3, Tables 3, 7, and Tables S₇, and S₁₀ (**Supporting Information**)], (phenylhydrazinylidene)propanedinitriles [compounds **63-67**, Scheme 4,

Tables 4, 7, and Table S₄ (**Supporting Information**), 4-arylazo-3,5-diamino-1*H*-pyrazoles [compounds **68-72**, Scheme 5, Table 5 and Table S₅ (**Supporting Information**)], and (*E,E*)-4-amino-1-aryl-3-cyano-4-methoxy-2-azabutadienes (compounds **73-75**, Scheme 6, Table 6).

2 MATERIALS AND METHODS

Materials and methods for Chemistry and Pharmacology are reported in Supporting Information. Caution: Storage and safety working conditions regarding malononitrile, arylidenemalononitriles and some nitrile-containing chemicals are mentioned in Supporting Information.

3 RESULTS AND DISCUSSION

3.1 Chemistry

3.1.1 Synthesis of arylidenepropanedinitriles

Arylidenepropanedinitriles **3** (compounds **16-41**) (Scheme 1) were synthesized by straightforward Knoevenagel condensation of the respective aldehyde **1** with malononitrile (**2**) (Gazit et al, 1989). Most compounds are common starting materials or intermediates in chemical reactions (Zayed et al., 1991; Marco et al., 2004; Ding & Zhao, 2010). Interesting results were also made known regarding their capacity to activate cell resistance to oxidative stress (Turpaev et al., 2011). Here we report the MAO and AChE inhibitory properties of a few arylidenepropanedinitriles and chemical data of the new arylidenepropanedinitriles **31**, **34**, **35** and **36** (Scheme 1; Figure 1).

Scheme 1 here

3.1.2 Synthesis of [(phenylamino)methylidene]propanedinitriles

[(Phenylamino)methylidene]propanedinitriles type **6** (compounds **42-52**) (Scheme 2) were readily synthesized by the reaction of malononitrile **2** with ethyl orthoformate **4** and the respective aniline derivative **5** (Wolfbeis, 1981). The MAO and AChE inhibitory activities are reported here as well as the data for the new [(phenylamino)methylidene]propanedinitrile derivatives **45**, **48**, and **52** (Scheme 2; Figure 1).

Scheme 2 here

3.1.3 Synthesis of 4-amino-1-phenyl-1*H*-pyrrole-3-carbonitriles and 3-amino-1-phenyl-1*H*-pyrrole-2,4-dicarbonitriles

The syntheses of both 4-amino-1-phenyl-1*H*-pyrrole-3-carbonitriles (compounds **53-57**) and 3-amino-1-phenyl-1*H*-pyrrole-2,4-dicarbonitriles (compounds **58-62**) are represented in Scheme 3 (compounds type **8**). These syntheses were based on a Thorpe-Ziegler cyclization via intermediate **7** using [(phenylamino)methylidene]propanedinitrile derivatives **6** as precursors (Scheme 2), an α -halo compound (chloroacetonitrile,

chloroacetone, ethyl bromoacetate, α -bromoacetophenone) and triethylamine. (Salaheldin et al., 2008; Unverferth et al., 1998; Salaheldin et al., 2010). Pharmacological data are reported concerning MAO inhibitory activities of type **8** compounds. Additionally, chemical data are addressed to the new compounds **59** and **60** (Scheme 3; Figure 1).

Scheme 3 here

3.1.4 Synthesis of (phenylhydrazinylidene)propanedinitriles

Phenylhydrazonomalononitriles **11** (compounds **63-67**) (Scheme 4) were prepared by diazotization of the appropriate arylamine **9**, followed by condensation of the diazonium salt **10** with malononitrile (Krystof et al., 2006). Compounds **63** (Krystof et al., 2006), **64** (Gavlik et al., 2017), **65** (Amer et al., 2004) and **66** (Tsai & Wang, 2005) are reported in the literature while (phenylhydrazinylidene) propanedinitrile **67** (Scheme 4) is a new compound which is described here for the first time. Pharmacological data are reported concerning MAO inhibitory activities of compounds type **11**. Additionally, chemical data are provided for the new compound **67** (Scheme 4; Figure 1).

Scheme 4 here

3.1.5 Synthesis of 4-arylo-3,5-diamino-1*H*-pyrazoles

The 4-arylo-3,5-diamino-1*H*-pyrazoles **12** (compounds **68-72**) were obtained by cyclocondensation of phenylhydrazonomalononitriles **11** (compounds **63-67**) with hydrazine (Krystof et al., 2006). Compounds **68** (Krystof et al., 2006; Al-Afaleq, 2000; Elgemeie et al., 2001), **69** (Al-Afaleq, 2000; Elgemeie et al., 2001), **70** (Huppertz et al., 1981), and **71** (Zhang et al., 2001) are reported in the literature while diaminopyrazole **72** (Scheme 5; Figure 1) is described here for the first time.

Scheme 5 here

3.1.6 Synthesis of (*E,E*)-4-amino-1-aryl-3-cyano-4-methoxy-2-azabutadienes

The (*E,E*)-4-amino-1-aryl-3-cyano-4-methoxy-2-azabutadienes **15** (compounds **73-75**) (Scheme 6) were synthesized by reaction of benzaldehyde (**13**: X=H) or its derivatives with aminomalononitrile *p*-toluenesulfonate (**14**) (Scheme 6) (Gutch et al., 2001). The synthesis of compound **73** is reported (Gutch et al., 2001). Compounds **74** and **75** (Scheme 6) are new. Here we report the chemical data and the MAO inhibitory activities for the new compounds **74** and **75** (Scheme 6; Figure 1).

Scheme 6 here

Figure 1 represents the chemical structures of all the new compounds (**31, 34, 35, 36, 45, 48, 52, 59, 60, 67, 72, 74, 75**).

Figure 1 here

3.1.7 Diverse pyrazole derivatives (compounds **76-81**) (Silva et al., 2010, Silva et al., 2011) and (phenoxyalkoxybenzylidenemalononitriles (compounds (**81**, **82**) (Silva et al., 2013) were previously synthesized and their AChE inhibitory activities reported. Here we describe their inhibitory activities in rat mitochondria (rMAO A and rMAO B) (Table S₂, Supporting Information).

3.2 Pharmacology

3.2.1 Monoamine oxidase inhibition

Compounds were screened for MAO inhibition using various assays: direct radiometric (rat mitochondrial MAO) or spectrophotometric (purified human MAO) assays or coupled fluorescent assays (any preparation). Initial screening was performed at fixed concentrations (10 or 25 μM) with $2xK_M$ substrates. Where inhibition greater than 70% was observed, IC_{50} values were measured. The IC_{50} values for selected inhibitors were re-evaluated in the coupled assay with horseradish peroxidase, measuring the fluorescence of resorufin produced in the presence of $2xK_M$ tyramine as substrate.

Table 1 shows IC_{50} values for purified human MAO A obtained using the spectrophotometric assay with kynuramine as the substrate. For the arylidenepropanedinitrile derivatives, an electron-rich substituent (F, Cl, NO_2) at the *para* position is detrimental to inhibition, although *m*- NO_2 is tolerated. Methoxy and propenyloxy substituents in the *para* position increase binding (**19**, **22**) but the benzyl ring substituent in **23** prevents binding. Changing the core benzyl ring to furan gives better inhibition (**30**, **31** and **32**).

Table 1 here

Only one of the [(phenylamino)methylidene]propanedinitrile derivatives was active, presumably due to interactions conferred by the *m*- NO_2 group (**49** in Table 2).

The phenylpyrrole mono- and dicarbonitriles (Table 3) were likewise poor inhibitors with only the dicarbonitrile **60** active with an IC_{50} of 6.2 μM .

The (phenylhydrazinylidene)propanedinitrile derivatives **63-67** (Table 4) were more promising with 5 active compounds. Methyl substitution in **67** was not good but the parent compound **65**, the *p*-Cl **66** and di-methoxy **64** derivatives gave IC_{50} values around 10 μM . The best inhibitor in this series was **63**, the *m*- NO_2 compound with an IC_{50} value of 1.65 μM .

Switching the dinitrile to a pyrazole group (Table 5) did not improve inhibition. The only active compound, the *p*-Cl derivative **69** was not much changed from the *p*-Cl derivative in the dinitrile series (**66** in Table 4).

Similarly, for the aminomethoxy compounds in Table 6, only one active compound was found. The 4-CN derivative **75** gave an IC_{50} value of 1.92 μM against human MAO A, 100 times better than the parent compound **73**.

Table 2 here

Table 3 here

Table 4 here

Table 5

Table 6 here

Since behavioral tests are performed on rodents, some compounds were also evaluated on MAO A and MAO B present in rat liver mitochondria (RLM) as presented in the Supplementary Information. Table S1 shows the IC₅₀ values for arylidenepropanedinitrile derivatives on RLM, assaying MAO A with [¹⁴C]-serotonin (5-HT) and MAO B with [¹⁴C]-β-phenylethylamine (PEA). Although **16**, **20**, and **26** were poor inhibitors as in purified hMAO A (around 60 μM, Table 1), **20** with two methoxy substituents was a better inhibitor than the others in the RLM MAO A assay (IC₅₀ 15.9 μM). Compounds **24** and **25** also gave similar IC₅₀ values against both human and rat MAO A. The RLM study allows direct comparison of selectivity between MAO A and B (Table S1). Although both **19** and **20** inhibit RLM MAO A, the extra *m*-OCH₃ in **20** removed the inhibition of MAO B seen with the mono-OCH₃ compound (**19**), making **20** selective for MAO A. The *m*-NO₂ derivative (**25**) is the best non-selective inhibitor of rat MAO, but moving the NO₂ to the *para* position (**24**) makes the compound selective for MAO B. Thus, in rat **25** is non-selective whereas **20** is MAO A-selective and **24** is B-selective, suggesting that discrimination is based on fine steric or electronic interaction in the active sites. None of the pyrazole derivatives (compounds **76-81**) and the phenoxyalkoxybenzylidenemalononitriles (compounds **81**, **82**) shown in Table S2 inhibited rMAO in RLM, but the arylidenepropanedinitrile series in Table S3 revealed some inhibition. rMAO A was inhibited by the rigid **40** (IC₅₀ = 18 μM) but more effectively by the flexible structures in **22** (3.5 μM) and **30** (0.72 μM). These compounds also inhibited rMAO B. The most effective on rMAO B were **23** (1.2 μM), and **28** (7.5 μM), neither of which inhibited MAO A in rat mitochondria.

Returning to human MAO, the inhibition of MAO A and MAO B was compared for several compound series using the coupled assay for hydrogen peroxide production. Table S4 reports the % inhibition at 25 μM and IC₅₀ values for (phenylhydrazinylidene)propanedinitrile compounds. Although di-methoxy substitution in **64** gives equal inhibition of MAO A (IC₅₀ = 22 μM) and MAO B (25 μM), the *m*-NO₂ (**63**) is 10 times better against MAO B (0.52 μM) than against MAO A (5.8 μM). In the same range (IC₅₀ values less than 10 μM), but non-selective, are **68-72** in Table S5, showing that the diaminopyrazole ring gives better inhibition than the dinitriles (**63-67** in Table S4). Table S6 confirms poor inhibition of human MAO by [(phenylamino)methylidene]propanedinitriles with none inhibiting MAO A and only two

inhibiting MAO B (**45** at 4.27 μM and **52** at 1.66 μM). Table S7 shows that the 4-amino-1-phenyl-1*H*-pyrrole-3-carbonitriles did not inhibit human MAO B, but some of the dicarbonitriles inhibited by about 50% at 25 μM . Dicarbonitrile **60** did not inhibit MAO B but was the only compound in Table S7 that inhibited MAO A (44%). Table S8 identified two arylidenepropanedinitriles that almost completely inhibited MAO A at 25 μM , namely **31** and **32** that share a furan linker.

Some compounds were also screened for inhibition of AChE (commercially cloned and purified electric eel AChE) at 10 μM and 5 μM (arylideneopropanedinitriles in Table S9 and phenylpyrrole aminocarbonitriles in Table S10). Only arylidenepropanedinitrile **37** (58% at 5 μM) and the phenylpyrrole-aminodicarbonitrile **62** (69% at 10 μM) gave inhibition. Otherwise these series were not inhibitory towards AChE.

Thus, compound **31** presents a lead for trifunctional inhibition against MAO A, MAO B and AChE (Table 7), while **32** offers a lead for selective MAO A inhibition coupled to AChE inhibition.

Table 7 here

After the primary screening in Tables 1-6 and Tables S1-S10 in Supplementary Information, a set of compounds was re-evaluated against all three human enzyme targets. Table 7 summarizes the IC_{50} values for the human MAO and AChE enzymes with the selected set of active compounds. Adding a nitrogen to the linker between the phenyl ring and the dicarbonitrile group (**25** vs **49**) loses MAO A inhibition but adding two nitrogens (**63**) improves inhibition of both MAO A and B and introduces some weak inhibition of AChE ($\text{IC}_{50} = 44 \mu\text{M}$). A furan linker again gives best lead compounds: **31** is a good inhibitor of both MAO A (0.34 μM) and MAO B (0.26 μM), whereas the trifluoro derivative (**32**) is 100-fold selective for MAO A (0.12 μM vs 15 μM for MAO B). Both **31** and **32** show some inhibition of AChE (IC_{50} values of 52 and 48 μM , respectively), so are lead compounds to optimize for multi-target activity.

3.2.2. Thioflavin T (ThT) assay to study A β aggregation

For this assay four arylidenepropanedinitriles (**31**, **32**, **33**, **37**), two (phenylhydrazinylidene)propanedinitriles (**63**, **65**), and one representative of (*E,E*)-4-amino-1-aryl-3-cyano-4-methoxy-2-azabutadienes (**75**) were chosen. The capacity of these compounds to inhibit the formation of A β_{1-42} fibrils (generated as described in Experimental section (**Supporting Information**)) was evaluated using the thioflavin T (ThT) fluorescence assay. This assay measures changes in fluorescence intensity of ThT upon binding to amyloid fibrils (Le Vine, 1999; Sulatskaya et al., 2012).

Figure 2 here

As can be seen in Figure 2, different concentrations (20, 40 and 60 μM) of compounds **31** (*p*-OCH₃ electron donating group and a *m*-Cl electron withdrawing group) and **32** (*m*-CF₃ strong electron withdrawing group) slightly inhibited the formation of A β_{1-42} fibrils, by about 25% and an insignificant 15%, respectively.

The pyrrole derivatives **33** and **37** (Figure 2) differed only in the C₅-CN electron withdrawing group in **37**. Both compounds were ineffective in disaggregating A β_{1-42} fibrils formation, being less adequate than **31** and **32** (Figure 2).

By contrast, compounds **63** and **65** (Figure 3), which differ only in the *m*-NO₂ electron withdrawing group present in **63**, were able to disaggregate Aβ₁₋₄₂ fibrils. The most effective was **63** (inhibitor effect of 50-60%, depending on the concentration), whereas **65** (Figure 3), and **75** (Figure 3) (*p*<0.05) inhibited Aβ aggregation only at high concentrations (40 and 60 μM).

Figure 3 here

3.2.3 Computational chemistry studies

3.2.2.1 Docking studies on monoamine oxidases

For our study we chose the derivatives **25**, **30**, **31**, **32**, **49**, **63**, and **65**. From these compounds only **49**, **63** and **65** form tautomers with the most probable ones shown in Figure 4. The binding energies values obtained for individual structures with MAO A and MAO B are represented in Table 8.

Figure 4 here

Table 8 here

The analysis of the inhibitor locations in the MAO A model provided several common features. If present, it is the nitro group which appears to be responsible for the interaction of the active derivatives (Figure 5). The comparison of the structurally similar compounds **49**, **63** and **65** showed that two inhibitors (**49** and **63**) directed the nitro group towards FAD, whereas for **65** (no nitro group) the dicyanonitrile group is directed towards FAD.

Figure 5 here

The main type of the interaction between the active inhibitor and FAD is a cation-π relationship, which is a kind of electrostatic interrelation (cation-quadrupole). Positive charge is located at nitrogen of nitro group and the π orbital is located at FAD; partial (but much lower) positive charge is located on the central carbon connected to the dicyano group (Figure 6). The value of the positive charge is also affected by other substituents, e.g. for **49** the atomic charge N (nitro) is diminished to 0.713 (Figure 7).

Figure 6 here

Figure 7 here

These specific features impacted the values of total binding energies (Table 8), which were higher for compound **63** due to a shorter distance from FAD (3.5 Å for **63** and 3.7 Å for **49**) as well as two additional interactions more (cation- π interaction with Tyr407 and hydrophobic interaction with Tyr444).

Another important factor affecting the ligand interaction is the presence and location of water molecules. The original ligand harmine has water molecules near it in the binding site. The docking procedure including water molecules is rather peculiar, so water was included after docking in the procedure of complex optimization. The addition of water was important to explain the lower activity of **30** (Figure S1). Although it interacts with Gln215, binding of **30** is hindered by more effective interaction of water molecule (HOH5342) with FAD.

Inspecting the binding modes of the strongest MAO A inhibitors **31** and **32** (Figure 8), it can be seen that the benzene ring of **31** is situated near the aromatic cleft of TYR 407 and TYR 444, but the malononitrile group of **32** is more deeply immersed into this region, at a distance of 2.99 Å from C10a of flavin. Docking and optimization studies provided two preferred orientations for both compounds: one with the malononitrile group near flavin and the second one with opposite direction. It seems that it is the substitution on the benzene ring which specifies the orientation of arylidenepropanedinitriles **31** and **32** as well as that for the (phenylhydrazinylidene)propanedinitriles **63**, **65** and [(phenylamino)methylidene]propanedinitrile **49**. Nitro and methoxy groups in positions *meta* and *para* of the benzene ring create sufficiently strong interactions with flavin or the aromatic cleft of the catalytic center while trifluoromethyl or no substitution permits the molecule to turn malononitrile group towards flavin. The abundant numbers of attractive interactions of **31** and **32** are reflected in values of binding energy (Table 8).

The inhibition activities of compounds **31** and **32** in MAO B were different from those in MAO A. The activity of **31** stayed almost the same, while IC₅₀ for **32** decreased in two orders from 0.12 μ M to 15.2 μ M. (Table 7). Docking calculations and subsequent optimization revealed the opposite orientation of the molecule **31** in MAO B compared with MAO A (Figures 8 and 9).

Figure 8

Figure 9 here

Both compounds interact with the gating residues Ile199 and Tyr326, which separate entrance and substrate cavities in MAO B (Milczek et al., 2011). However, in MAO B, the position of the conjugated malononitrile groups in the vicinity of the aromatic cleft was strengthened by close contact of one cyano nitrogen with hydroxyl group of Cys172 for **31** and by the interaction with internal water near FAD for **32**. Due to the surrounding

residues and water, the furan ring and the malonitrile group of **32** are visibly turned against the substituted benzene ring (sum of both deviations is 44°). This fact breaks the conjugation in **32** and, finally, penalizes the position of **32** in MAO B when compared with **31**, which is turned less (22°).

The water molecules can provide additional interactions for ligand and stabilize or destabilize its position. Water found in the binding of **32** in MAO B pocket is positionally similar to the water molecule participating in catalysis. So far, there has been no structural work on MAO to show the positioning of ligands with the malonitrile group in the active site.

A similar binding mode can be observed for **63**. This compound is depicted in Figure S2 for the binding sites of MAO A and MAO B. The nitro group of **63** adjacent to FAD in both types of MAO is preferred, although for both enzymes reverse positions also exist (Figure S3). but with lower values of binding energy. (The differences in values of binding energy were 20.5 kJ/mol for MAO A and 4.3 kJ/mol for MAO B.). Compound **63** is bound in MAO A with Tyr407 by π - π and cation- π interaction and with FAD by cation- π interaction with distance 4.1 Å. The position is stabilized by H-bonds with Phe208 and one surrounding water molecule, as well as a hydrophobic interaction with Gln215. However, both H-bonds make the position less energetically favorable due to the twisting of malonitrile group. Interaction with Phe208 in MAO A or Ile199 in MAO B has been related to selectivity of compounds either in the role of inhibitors (Morón et al., 2000) or as substrates (Tsugeno & Ito, 1997). The stronger inhibition of MAO B with **63** was visualised as a firm position of nitro group between Tyr398 and Tyr435, H-bond with Tyr188 and π - π edge-to-edge interaction with FAD (distance 3.7 Å). The malonitrile group is held by a single H-bond with a water molecule occurring in the cavity. The resulting position keeps the whole molecule in one plane, contributing thus to the overall benefit of this mode of interaction.

For further work, the affinity of **63** towards MAO B could be enhanced by a proper substitution in 2 or 3 position from the nitro group. An interesting study would be made with a thiol substitution, as in the proximity of these two places there is Cys172, which could thus create a disulfide bond with the ligand. Another possibility would be to introduce a benzyl or phenyl group in position 1, to obtain the π - π interaction with Tyr435.

3.2.2.2 Docking studies on acetylcholinesterase

Docking and optimization calculations were performed to determine the binding mode of ligands to AChE for compounds **32** (Table S9), **37** (Table S9, Figure S4), **62** (Salaheldin et al., 2008) (Table S10), **82** [IC_{50} (AChE) = $6.0 \pm 0.5 \mu\text{M}$] (Silva et al. 2013), (Table S2, Figures 10, 11), and **83** [IC_{50} (AChE) = $2.1 \pm 0.5 \mu\text{M}$] (Silva et al. 2013) (Table S2, Figures 10, 11). In the figures, all the compounds are rendered as balls and sticks. The side chains conformations of the mobile residues are illustrated in the same color (light blue) as the ligand. Different subsites of the active site are colored as follows: catalytic triad (CT) in green, oxyanion hole (OH) in pink, anionic subsite (AS) in orange except Trp86, acyl binding pocket (ABP) in yellow, peripheral anionic site (PAS) in cyan and the non-active site residues in grey. Hydrogen bonds are represented as yellow dashed lines, π - π interactions as red lines, π -cation interactions as blue lines and hydrophobic contacts as green ones.

Figure 10 here

Figure 11 here

Table S12 summarizes the values of binding energy (E_{bin}) together with the inhibition activities of the chosen compounds. The binding energy values for **32** and **62** correspond to their lower activities, but **37** should be as strong inhibitor as **82** and **83** according to E_{bin} value. This compound is immersed in the ligand cavity with both malononitrile and cyano groups (Figure S4) bound to Trp86 (π - π interaction), Phe297 (hydrophobic) and Glu204 (H-bond). According to these interactions, **37** should be much stronger inhibitor than it was measured. The reason for its lower activity could be found in the value of the solvation energy (Table S11), which is very low and thus represents quite a big value of desolvation penalty in total ligand binding.

Compounds **82** and **83** contain long aliphatic chains and, for both, the malononitrile group represents the hydrophilic part in a generally hydrophobic molecule (Figure 12), which can be observed also in values of solvation energy (Table S11). The length of the aliphatic chain fits in the cavity of hAChE more comfortable for **83** than for **82** (Figure 10). Both compounds are anchored to the cavity by strong interaction between malononitrile group and Trp236 from the PAS region. Malononitrile groups, directed to the outer space, are also bound with surrounding water molecules (Figure 11). The compounds fill major parts of the ligand cavity, **83** more than **82**. (Figure 11).

Figure 12 here

4 CONCLUSIONS

In this paper we have reported the synthesis and biological evaluation of 83 compounds, 13 of which are new. Based on the MAO inhibition properties of the carbonitrile group we carried out a systematic exploration to discover new classes of nitrile-containing

compounds endowed with dual AChE and MAO inhibitory activities, and A β anti-aggregating properties. Thus, arylidenepropanedinitriles, [(phenylamino)methylidene]propanedinitriles, 4-amino-1-phenyl-1*H*-pyrrole-3-carbonitriles, 3-amino-1-phenyl-1*H*-pyrrole-2,4-dicarbonitriles, (phenylhydrazinylidene)propanedinitriles, 4-arylo-3,5-diamino-1*H*-pyrazoles and (*E,E*)-4-amino-1-aryl-3-cyano-4-methoxy-2-azabutadienes were synthesized and assessed.

From *in vitro* screening, compound **31** presents the best lead for trifunctional inhibition against MAO A, MAO B and AChE (Table 7), while **32** offers a lead for selective MAO A inhibition coupled to AChE inhibition.

Computational analysis of the binding modes of the compounds demonstrated several characteristic features. The malononitrile group, when not overcome by more attractive groups as nitro or methoxy groups, can find an advantageous position with the aromatic cleft and FAD of MAO A or MAO B. The total binding energy can be handicapped by an internal penalty caused by twisting of ligand molecule and subsequent disruption of the conjugation as happens in **32** with MAO B compared to the conjugated **31**. Conjugation is also important for AChE. In addition, the hydrophilic character of malononitrile allows this group to be in close contact with the water environment in the more open binding pocket of AChE, as seen for **83** in AChE.

Although the effect of **31** and **32** against A β ₁₋₄₂ was very weak, the effect of the other compounds was quite comparable to the action observed for resveratrol (20 μ M), used as a reference disaggregating compound (Silva et al. 2013). Overall, the data indicated that compounds **63**, **65** and **75** (Figure 3) were able to disaggregate A β ₁₋₄₂ fibrils. The most effective was **63**, a (phenylhydrazinylidene)propanedinitrile derivative that also inhibited MAO A at micromolar concentration, making it a potential lead for Alzheimer's disease application.

CONFLICT OF INTEREST

The authors declare no conflict of interest in this research work.

SUPPORTING INFORMATION

Additional supporting information may be found online in the Supporting Information section at the end of this article.

ORCID

M. Carmo Carreiras: <https://orcid.org/0000-0001-7096-2449>

Rona R. Ramsay: <http://orcid.org/0000-0003-1535-4904>

REFERENCES

- Aiai, M., Robert, A., Baudy-Floc'h, M., & Le Grel, P. (1995). First sharpless epoxidation of electrophilic 2-cyanoallylic alcohols. *Tetrahedron Asymmetry*, 6(9), 2249-2252.
- Al-Afaleq, E.I. (2000). Heterocyclic synthesis via enamionitriles: an efficient, one step synthesis of some novel azolo[1,5- α]pyrimidine, pyrimido[1,2- α]benzimidazole, pyrido[1,2- α]benzimidazole, pyrimidine and pyrazole derivatives. *Synthetic Communications*, 30(11), 1985-1999.
- Alvarez, A., Alarcón, R., Opazo, C., Campos, E.O., Muñoz, F.J., Calderón, F.H., ...Inestrosa, N.C. (1998). Stable complexes involving acetylcholinesterase and

- amyloid- β -peptide change the biochemical properties of the enzyme and increase the neurotoxicity of Alzheimer's fibrils. *Journal of Neuroscience*, 18(9), 3213-3223.
- Alvarez, A., Opazo, C., Alarcón, R., Garrido, J., & Inestrosa, N.C. (1997). Acetylcholinesterase promotes the aggregation of amyloid- β -peptide fragments by forming a complex with the growing fibrils. *Journal of Molecular Biology*, 272, 348-361.
- Amer, A.M., El-Mobayed, M.M., & Asker, S. (2004). On the chemistry of cinnoline V [1]. Reactions of 4-aminocinnolines with amines. *Monatshefte für Chemie*, 135, 595-604.
- Arendt, T., Brückner, M.K., Lange, M., & Bigl, V. (1992). Changes in acetylcholinesterase and butyrylcholinesterase in alzheimers-disease resemble embryonic-development – a study of molecular forms. *Neurochemistry International*, 21, 381-396. Doi: 10.1016/0197-0186(92)90189-X.
- Bortolato, M., & Shih, J.C. (2011). Behavioral outcomes of monoamine oxidase deficiency: preclinical and clinical evidence. *International Review of Neurobiology*, 100, 13-42.
- Boyd, M.J., Crane, S.N., Robichaud, J., Scheiget, J., Black, W.C., Chauret, N., ...Oballa, R.M. (2009). Investigation of ketone warheads as alternatives to the nitrile for preparation of potent and selective cathepsin K inhibitors. *Bioorganic & Medicinal Chemistry Letters*, 19, 675-679.
- Cai, Z. (2014). Monoamine oxidase inhibitors: promising therapeutic agents for Alzheimer's disease (Review). *Molecular Medicine Reports*, 9, 1533-1541.
- Chirkova, Z.V., Kabanova, M.V., Filimonov, S.I., Abramov, I.G., Petzer, A., Petzer, J.P., ...Suponitsky, K.Y. (2015). Inhibition of monoamine oxidase by indole-5,6-dicarbonitrile derivatives. *Bioorganic & Medicinal Chemistry Letters*, 25, 1206-1211.
- Das, S., & Basu, S. (2017). Multi-targeting strategies for Alzheimer's disease therapeutics: pros and cons. *Current Topics in Medicinal Chemistry*, 17(27), 3017-3061.
- Davison, A. N. (1957). The mechanism of the irreversible inhibition of rat-liver monoamine oxidase by iproniazid (Marsilid). *The Biochemical Journal*, 67, 316-322.
- De Ferrari, G., Canales, M.A., Shin, I., Weiner, L.M., Silman, I., Inestrosa, N.C. (2001). A structural motif of acetylcholinesterase that promotes amyloid- β -peptide fibril formation. *Biochemistry*, 40, 10447-10457.
- Ding, D., & Zhao, C.-G. (2010). Organocatalyzed synthesis of 2-amino-8-oxo-5,6,7,8-tetrahydro-4H-chromene-3-carbonitriles. *Tetrahedron Letters*, 51(9), 1322. Doi:10.1016/j.tetlet.2009.12.139.
- Elgemeie, G.H., El-Ezbawy, S.R., & Ali, H.A. (2001). Reactions of chlorocarbonyl isocyanate with 5-aminopyrazoles and active methylene nitriles: a novel synthesis of pyrazolo[1,5-*a*]-1,3,5-triazines and barbiturates. *Synthetic Communications*, 31(22), 3459-3467.
- Fleming, F.F., Yao, L., Ravikumar, P.C., Funk, L., & Shook, B.C. (2010). Nitrile-containing pharmaceuticals: efficacious roles of the nitrile pharmacophore. *Journal of Medicinal Chemistry*, 53(22), 7902-7917.
- Gauthier, J.Y., Chauret, N., Cromlish, W., Desmarais, S., Duong, Le T., Falguyret, J.-P., ...Black, W.C. (2008). The discovery of odanacatib (MK-0822), a selective inhibitor of cathepsin K. *Bioorganic & Medicinal Chemistry Letters*, 18, 923-928.

- Gavlik, K.D., Sukhorukova, E.S., Shafran, Y.M., Slepukhin, P.A., Benassi, E., & Belskaya, N.P. (2017). 2-aryl-5-amino-1,2,3-triazoles: new effective blue-emitting fluorophores. *Dyes and Pigments*, *136*, 229-242.
- Gazit, A., Yaish, P., Gilon, C., & Levitski, A. (1989). Tyrphostins I: Synthesis and biological activity of protein tyrosine kinase inhibitors. *Journal of Medicinal Chemistry*, *32*(10), 2344-2352.
- Gutch, P.K., Raza, S.K., & Malhotra, R.C. (2001). Synthesis, characterization and mass spectrometric fragmentation of *gem*-dicyanooxiranes derived from benzylidene malononitrile. *Indian Journal of Chemistry*, *40B*, 243-247.
- Hideji, T. & Kazuo, H. (1984). Studies on the mechanism of acute toxicity of nitriles in mice. *Archives of Toxicology*, *55*, 47-54.
- Hideji, T. & Kazuo, H. (1986). Influence of ethanol on the in vivo and in vitro metabolism of nitriles in mice. *Archives of Toxicology*, *58*(3), 171-176.
- Hroudova, J., Singh, N., Fisar, Z., & Ghosh, K.K., (2016). Progress in drug development for Alzheimer's disease: an overview in relation to mitochondrial energy metabolism. *European Journal of Medicinal Chemistry*, *121*, 774-784.
- Huppatz, J.L., Phillips, J.N., & Rattigan, B.M. (1981). Cyanoacrylates: Herbicidal and Photosynthetic inhibitory activity. *Agricultural and Biological Chemistry*, *45*(12), 2769-2773.
- Inestrosa, N.C., Alvarez, A., Pérez, C.A., Moreno, R.D., Vicente, M., Linker, C., ...Garrido, J. (1996). Acetylcholinesterase accelerates assembly of amyloid- β -peptides into Alzheimer's fibrils: possible role of the peripheral site of the enzyme. *Neuron*, *16*, 881-891.
- Jakob-Roetne, R. & Jacobsen, H. (2009). Alzheimer's disease: from pathology to therapeutic approaches. *Angewandte Chemie International Edition*, *48*(17), 3030-3059.
- Johnson, G., & Moore, S.W. (1999). The adhesion function on acetylcholinesterase is located at the peripheral anionic site. *Biochemical Biophysical Research Communications*, *258*, 758-762.
- Jones, L.H., Summerhill, N.W., Swain, N.A., & Mills, J.E. (2010). Aromatic chloride to nitrile transformation: medicinal and synthetic chemistry. *Medicinal Chemistry Communications*, *1*, 309-318.
- Juárez-Jiménez, J., Mendes, E., Galdeano, C., Martins, C., Silva, D.B., Marco-Contelles, J., Carreiras, M.C., ...Ramsay, R.R. (2014). Exploring the structural basis of the selective inhibition of monoamine oxidase A by dicyanitrile aminoheterocycles: role of Asn181 and Ile355 validated by spectroscopic and computational studies. *Biochimica et Biophysica Acta*, *1844*, 389-397.
- Kennedy, B.P., Ziegler, M.G., Alford, M., Hansen, L.A., Thal, L.J., & Masliah, E. (2003). Early and persistent alterations in prefrontal cortex – MAO A and B in Alzheimer's disease. *Journal of Neural Transmission*, *110*, 789-801.
- Korabecny, J., Nepovimova, E., Cikankova, T., Spilovska, K., Vaskova, L. ...Hroudova, J. (2018). Newly developed drugs for Alzheimer's disease in relation to energy metabolism, cholinergic and monoaminergic neurotransmission. *Neuroscience*, *370*, 191-206.
- Krystof, V., Cankar, P., Frysova, I., Slouka, J., Kontopidis, G., Dzubak, P., ...Strnad, M. (2006). 4-aryloxy-3,5-diamino-1H-pyrazole CDK inhibitors: SAR study, crystal structure in complex with CDK2, selectivity, and cellular effects. *Journal of Medicinal Chemistry*, *49*(22), 6500-6509.

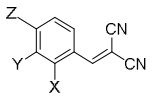
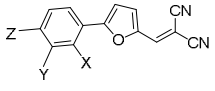
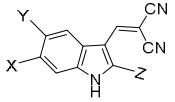
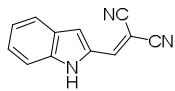
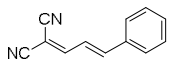
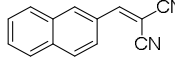
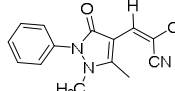
- Kudoh, S. (1990). Direct determination of the antihypertensive agent cromakalim and its major metabolites in human urine by high-performance liquid chromatography. *Journal of Chromatography*, *515*, 597-602.
- Kudoh, S., Okada, H., Nakahira, K., & Nakamura, H. (1990). Simultaneous determination of antihypertensive agent cromakalim and its major metabolites in human urine by high performance liquid chromatography. *Analytical Sciences*, *6*, 53-56.
- LeVine, 3rd H. (1999). Quantification of β -sheet amyloid fibril structures with thioflavin T. *Methods in Enzymology*, *309*, 274-284.
- Lindsay-Scott, P.J., & Gallagher, P.T. (2017). Synthesis of heterocycles from arylacetonitriles: powerful tools for medicinal chemists. *Tetrahedron Letters*, *58*(27), 2629-2635.
- MacFaul, P.A., Morley, A.D., & Crawford, J.J. (2009). A simple in vitro assay for assessing the reactivity of nitrile containing compounds. *Bioorganic & Medicinal Chemistry Letters*, *19*, 1136-1138.
- Manley-King, C.I., Bergh, J.J., & Petzer, J.P. (2012). Monoamine oxidase inhibition by C4-substituted phthalonitriles. *Bioorganic Chemistry*, *40*, 114-124.
- Marco, J.L., de los Ríos, C., Garcia, A.G., Villarroja, M., Carreiras, M.C., Martins, C., ...Luque, F.J. (2004). Synthesis, biological evaluation and molecular modelling of diversely functionalized heterocyclic derivatives as inhibitors of acetylcholinesterase/butyrylcholinesterase and modulators of Ca^{2+} channels and nicotinic receptors. *Bioorganic & Medicinal Chemistry*, *12*, 2199-2218.
- McIlhenny, H.M. (1971). Metabolism of [^{14}C]Verapamil. *Journal of Medicinal Chemistry*, *14*(12), 1178-1184.
- Milczek, E.M., Binda, C., Rovida, S., Mattevi, A., & Edmondson, D.E. (2011). The "gating" residues Ile199 and Tyr326 in human monoamine oxidase B function in substrate and inhibitor recognition. *The FEBS Journal*, *278*(24), 4860-4869.
- Miyashita, M., Suzuki, T., & Yoshikoshi, A. (1987). Fluoride-promoted epoxidation of α,β -unsaturated compounds. *Chemistry Letters*, 285-288.
- Morón, J.A., Campillo, M., Perez, V., Unzeta, M., & Pardo, L. (2000). Molecular determinants of MAO selectivity in a series of indolylmethylamine derivatives: biological activities, 3D-QSAR/CoMFA analysis, and computational simulation of ligand recognition. *Journal of Medicinal Chemistry*, *43*(9), 1684-1691.
- Muñoz, F.J., & Inestrosa, N.C. (1999). Neurotoxicity of acetylcholinesterase amyloid β -peptide aggregates is dependent on the type of A β peptide and the AChE concentration present in the complexes. *FEBS Letters*, *450*(3), 205-209.
- Naoi, M., Maruyama, W., & Shamoto-Nagai, M. (2018). Type A and B monoamine oxidases distinctly modulate signal transduction pathway and gene expression to regulate brain function and survival of neurons. *Journal of Neural Transmission*, *125*, 1635-1650.
- Oballa, R.M., Truchon, J.-F., Bayly, C.I., Chauret, N., Day, S., Crane, S., & Berthelette, C. (2007). A generally applicable method for assessing the electrophilicity and reactivity of diverse nitrile-containing compounds. *Bioorganic & Medicinal Chemistry Letters*, *17*, 998-1002.
- Pryde, D.C., Henry, S.S., & Meyers, A.I. (1996). Synthesis of 2-tetralones via a novel 1,2-carbonyl transposition of 1-tetralones. *Tetrahedron Letters*, *37*(19), 3243-3246.
- Ramadan, Z.B., Wrang, M.L., & Tipton, K.F. (2007). Species differences in the selective inhibition of monoamine oxidase (1-methyl-2-phenylethyl)hydrazine and its potentiation by cyanide. *Neurochemical Research*, *32*, 1783-1790.
- Ramsay, R.R. (2016). Molecular aspects of monoamine oxidase B. *Progress in Neuro-Psychopharmacology & Biological Psychiatry*, *69*, 81-89.

- Ramsay, R.R., & Tipton, K. (2017). Assessment of enzyme inhibition: A review with examples from the development of monoamine oxidase and cholinesterase inhibitory drugs. *Molecules*, *22*, 1192. Doi: 10.3390/molecules22071192.
- Reyes, A.E., Chacón, M.A., Dinamarca, M.C., Cerpa, W., Morgan, C., & Inestrosa, N.C. (2004). Acetylcholinesterase-A β complexes are more toxic than A β fibrils in rat hippocampus. *American Journal of Pathology*, *164*(6), 2163-2174.
- Reznicek, J., Ceckova, M., Ptackova, Z., Martinec, O., Tupova, L., Cerveny, L., & Staud, F. (2017). MDR1 and BCRP transporter-mediated drug-drug interaction between rilipirine and abacavir and effect on intestinal absorption. *Antimicrobial agents and Chemotherapy*, *61*(9), e00837-17.
- Salaheldin, A.M., Oliveira-Campos, A.M.F., & Rodrigues, L.M. (2008). 3-aminopyrroles and their application in the synthesis of pyrrolo[3,2-*d*]pyrimidine (9-deazapurine) derivatives. *Arkivoc*, *xiv*, 180-190.
- Salaheldin, A.M., Oliveira-Campos, A.M.F., Parpot, P., Rodrigues, L.M., Oliveira, M.M., & Feixoto, F.P. (2010). Synthesis of new tacrine analogues from 4-amino-1*H*-pyrrole-3-carbonitrile. *Helvetica Chimica Acta*, *93*, 242-248.
- Samadi, A., Chioua, M., Bolea, I., de los Ríos, C., Iriepa, I., Moraleda, I., ...Marco-Contelles, J. (2011). Synthesis, biological assessment and molecular modeling of new multipotent MAO and cholinesterase inhibitors as potential drugs for the treatment of Alzheimer's disease. *European Journal of Medicinal Chemistry*, *46*, 4665-4668.
- Samadi, A., de la Fuente Revenga, M., Pérez, C., Iriepa, I., Moraleda, I., Rodríguez-Franco, M.I., & Marco-Contelles, J. (2013). Synthesis, pharmacological assessment, and molecular modeling of 6-*chloro-pyridonepezils*: new dual AChE inhibitors as potential drugs for the treatment of Alzheimer's disease. *European Journal of Medicinal Chemistry*, *67*, 64-74.
- Samadi, A., Estrada, M., Pérez, C., Rodríguez-Franco, M.I., Iriepa, I., ...Marco-Contelles, J. (2012). *Pyridonepezils*, new dual AChE inhibitors as potential drugs for the treatment of Alzheimer's disease: synthesis, biological assessment, and molecular modeling. *European Journal of Medicinal Chemistry*, *57*, 296-301.
- Samadi, A., Marco-Contelles, J., Soriano, E., Álvarez-Pérez, M., Chioua, M., Romero, A., González-Lafuente, L., Gandía, L., ...de los Ríos, C. (2010). Multipotent drugs with cholinergic and neuroprotective properties for the treatment of Alzheimer and neuronal vascular diseases. I. Synthesis, biological assessment, and molecular modeling of simple and readily available 2-aminopyridine-, and 2-chloropyridine-3,5-dicarbonitriles. *Bioorganic & Medicinal Chemistry*, *18*, 5861-5872.
- Samadi, A., Valderas, C., de los Ríos, C., Bastida, A., Chioua, M., González-Lafuente, L., ...Marco-Contelles, J. (2011). Cholinergis and neuroprotective drugs for the treatment of Alzheimer and neuronal vascular diseases. II. Synthesis, biological assessment, and molecular modelling of new tacrine analogues from highly substituted 2-aminopyridine-3-carbonitriles. *Bioorganic & Medicinal Chemistry*, *19*, 122-133.
- Schedin-Weiss, S., Inoue, M., Hromadkova, L., Teranishi, Y., Yamamoto, N.G., Wiehager, B., ...Tjerberg, L.O. (2017). Monoamine oxidase B is elevated in Alzheimer disease neurons, is associated with γ -secretase and regulates neuronal amyloid β -peptide levels. *Alzheimers Research Therapy*, *9*, 57. Doi: 10.1186/s13195-017-0279-1.
- Sharma, P., Srivastava, P., Seth, A., Tripathi, P.N., Banerjee, A.G., & Shrivastava, S. K. (2019). Comprehensive review of mechanisms of pathogenesis involved in

- Alzheimer's disease and potential therapeutic strategies. *Progress in Neurobiology*, *174*, 53-89.
- Silva, D., Chioua, M., Samadi, A., Agostinho, P., Garção, P., Lajarín-Cuesta, R., ...Carreiras, M.C. (2013). Synthesis, pharmacological assessment, and molecular modeling of acetylcholinesterase/butyrylcholinesterase inhibitors: effect against amyloid- β -induced neurotoxicity *ACS Chemical Neuroscience*, *4*, 547-565.
- Silva, D., Chioua, M., Samadi, A., Carreiras, M.C., Jimeno M.-L., Mendes, E., ...Marco-Contelles, J. (2011). Synthesis and pharmacological assessment of diversely substituted pyrazolo[3,4-*b*]quinoline, and benzo[*b*]pyrazolo[4,3-*g*][1,8]naphthyridine derivatives. *European Journal of Medicinal Chemistry*, *46*, 4676-4681.
- Silva, D., Samadi, A., Chioua, M., Carreiras, M.C., & Marco-Contelles, J. (2010). The Sandmeyer reaction on some selected heterocyclic ring systems: synthesis of useful 2-chloroheterocyclic-3-carbonitrile intermediates. *Synthesis*, *16*, 2725-2730.
- Singh, P.D.A., Jackson, J.R., & James S.P. (1985). Metabolism of mandelonitrile in the rat. *Biochemical Pharmacology*, *34*(12), 2207-2209.
- Strong, H.A., & Spino, M. (1987). Highly sensitive determination of cimetidine and its metabolites in serum and urine by high-performance liquid chromatography. *Journal of Chromatography*, *422*, 301-308.
- Sulatskaya, A.I., Kuznetsova, I.M., & Turoverov, K.K. (2012). Interaction of thioflavin T with amyloid fibrils: fluorescence quantum yield of bound dye. *Journal of Physical Chemistry B*, *116*(8), 2538-2544.
- Tsai, P.C., & Wang, I.J. (2005). Synthesis and solvatochromic properties of some disazo dyes derived from pyrazolo[1,5-*a*]pyrimidine derivatives. *Dyes and Pigments*, *64*, 259-264.
- Tsugeno, Y., & Ito, A. (1997). A Key Amino Acid Responsible for Substrate Selectivity of Monoamine Oxidase A and B. *Journal of Biological Chemistry*, *272*(22), 14033-14036.
- Turpaev, K., Ermolenko, M., Cresteil, T., & Drapier, J.C. (2011). Benzylidenemalonitrile compounds as activators of cell resistance to oxidative stress and modulators of multiple signaling pathways. A structure-activity relationship study. *Biochemical Pharmacology*, *82*, 535-547.
- Ugun-Klusek, A., Theodosi, T.S., Fitzgerald, J.C., Burté, F., Ufer, C., Boocock, D.J., ...Billet, E.E. (2019). Monoamine oxidase-A promotes protective autophagy in human SH-SY5Y neuroblastoma cells through Bcl-2 phosphorylation. *Redox Biology*, *20*, 167-181.
- Unverferth, K., Engel, J., Höfgen, N., Rostock, A., Günther, R., Lankau, H.-J., ...Hofmann, H.-J. (1998). Synthesis, anticonvulsant activity, and structure-activity relationships of sodium channel blocking 3-aminopyrroles. *Journal of Medicinal Chemistry*, *41*(1), 63-73.
- Unzeta, M., Esteban, G., Bolea, I., Fogel, W.A., Ramsay, R.R., Youdim, M.B.H., ...Marco-Contelles, J. (2016). Multi-target directed donepezil-like ligands for Alzheimer's disease. *Frontiers in Neuroscience*, *10*. Doi: 10.3389/fnins.2016.00205.
- Van deer Walt, M.M., Terre'Blanche, G., Lourens, A.C.U., Petzer, A., & Petzer, J.P. (2012). Sulphonylphthalonitrile analogues as selective and potent inhibitors of monoamine oxidase B. *Bioorganic & Medicinal Chemistry Letters*, *22*, 7367-7370.
- Vourvahis, M., Gleave, M., Nedderman, A.N.R., Hyland, R., Gardner, I., Howard, M., ...LaBadie, R. (2010). Excretion and metabolism of Lersivirine (5-{[3,5-diethyl-1-(2-hydroxyethyl)(3,5-¹⁴C₂)-1*H*-pyrazol-4-yl]oxy}benzene-1,3-dicarbonitrile), a

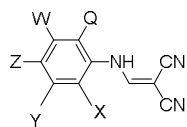
- next-generation non-nucleoside reverse transcriptase inhibitor, after administration of [¹⁴C]Lersivirine to healthy volunteers. *Drug metabolism and disposition*, 38, 789-800.
- Wang, H., & Zhang, H. (2019). Reconsideration of anticholinesterase therapeutic strategies against Alzheimer's disease. *ACS Chemical Neuroscience*, 10(2), 852-862.
- Wikberg, T., & Vuorela, A. (1994). Metabolite profiles of two [¹⁴C]-labelled catechol O-methyltransferase inhibitors, nitecapone and entacapone, in rat and mouse urine and rat bile. *European Journal of Drug Metabolism and Pharmacokinetics*, 19(2), 125-135.
- Wit, J.G., & van Genderen, H. (1966). Metabolism of the herbicide 2,6-dichlorobenzonitrile in rabbits and rats. *Biochemistry Journal*, 101, 698-706.
- Wolfbeis, O.S. (1981). Eine Eintopfsynthese von 3-amino-1H-pyrazol-4-carbonitril. *Monatshefte für Chemie*, 112, 875-877.
- Zayed, S.E., Elmaged, E.I.A., Metwally, S.A., & Elnagdi, M.H. (1991). Reactions of six-membered heterocyclic β-enaminotriles with electrophilic reagents. *Collection of Czechoslovak Chemical Communications*, 56(10), 2175-2182.
- Zhang, Z., Yan, J., Leung, D., Costello, P.C., Sanghera, J., Daynard, T.S., Wang, S., & Chafeev, M. (2001). Vancouver, CA Patent No. WO 01/77080, World Intellectual Property Organization, International Bureau.

TABLE 1 IC₅₀ values (μM) for inhibition of human MAO A by arylidenepropanedinitriles **16-41**

Compound	X, Y, Z	hMAO A IC ₅₀ (μM)
	16 X,Y,Z=H	60.7 ±11.4
	17 X,Y=H; Z=CH ₃	>100
	18 X=CH ₃ ; Y,Z=H	71.3 ±362
	19 X,Y=H; Z=OCH ₃	21.4 ±2.70
	20 X=H; Y,Z=OCH ₃	58.0 ±12.0
	21 X,Y,Z=OCH ₃	288.0 ±33.6
	22 X,Y=H; Z=OCH ₂ CHCH ₂	11.3 ±1.08
	23 X,Y=H; Z=OCH ₂ Ph	>100
	24 X,Y=H; Z=NO ₂	>100
	25 X,Z=H; Y=NO ₂	9.05 ± 0.091
26 X,Y=H; Z=Cl	68.9 ± 4.70	
27 X,Y=H; Z=F	258.0±68.8	
28 X,Y=H; Z=CN	27.4±7.40	
29 X=CN; Y,Z=H	>100	
	30 X,Y=H; Z=NO ₂	15.7±1.87
	31 X=H; Y=Cl; Z=OCH ₃	2.67±0.274
	32 X,Z=H; Y=CF ₃	1.43±0.265
	33 X,Y,Z=H	43.4±10.6
	34 X,Z=H; Y=OCH ₂ Ph	71.7±43.4
	35 X=Br; Y,Z=H	15.9±4.07
	36 X,Y=H; Z=CN	66.6±59.2
	37 X,Z=H; Y=CN	166.0±27.2
	38	27.2±4.47
	39	172.0±28.6
	40	13.7±1.06
	41	>100

IC₅₀ values were determined spectrophotometrically with kynuramine as substrate.

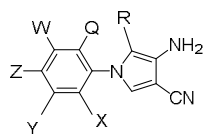
TABLE 2 IC₅₀ values (μM) for inhibition of human MAO A by [(phenylamino)methylidene]propanedinitriles **42-52**.



	X, Y, Z, W, Q	hMAO A IC₅₀ (μM)
42	X, Y, Z, Q, W=H	>100
43	X=CH ₃ ; Y, Z, Q, W=H	>100
44	X, Q=CH ₃ ; Y, Z, W=H	>100
45	X, Z, Q=CH ₃ ; Y, W=H	78.6±70.1
46	X, Z, Q=H; Y, W=CH ₃	109±72.6
47	X, W, Q=H; Y, Z=CH ₃	108±24.0
48	X, W, Q=H; Y, Z=OCH ₃	>100
49	X, Z, W, Q=H; Y=NO ₂	9.65±1.36
50	X, Y, W, Q=H; Z=Cl	>100
51	X, Z=Cl; Y, W, Q=H	>100
52	X, Q=CH ₃ ; Y, W=H; Z=Br	197±90.7

IC₅₀ values were determined spectrophotometrically with kynuramine as substrate.

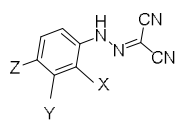
TABLE 3 IC₅₀ values (μM) for inhibition of human MAO A by 4-amino-1-phenyl-1*H*-pyrrole-3-carbonitriles **53-57** and 3-amino-1-phenyl-1*H*-pyrrole-2,4-dicarbonitriles **58-62**.



X, Y, Z, W, Q, R	hMAO A IC ₅₀ (μM)
53 X, Y, Z, W, Q=H; R=CO ₂ Et	36.2±6.91
54 X, Y, Z, W, Q=H; R=COCH ₃	>100
55 X, Y, W, Q=H; Z=Cl; R=CO ₂ Et	92.5±18.9
56 X, Y, W, Q=H; Z=Cl; R=COCH ₃	>100
57 X, Y, W, Q=H; Z=OCH ₃ ; R=CO ₂ Et	>100
58 X, Y, Z, W, Q=H; R=CN	1464±513
59 X, W, Q=H; Y, Z=CH ₃ ; R=CN	113±17.4
60 X, Z, Q=H; Y, W=CH ₃ ; R=CN	6.21±4.69
61 X, Y, W, Q=H; Z=Cl; R=CN	241±36.3
62 X, Y, W, Q=H; Z=OCH ₃ ; R=CN	>100

IC₅₀ values were determined spectrophotometrically with kynuramine as substrate.

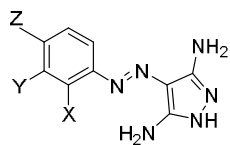
TABLE 4 IC₅₀ values (μM) for inhibition of human MAO A by (phenylhydrazinylidene)propanedinitriles **63-67**.



X, Y, Z	hMAO A IC₅₀ (μM)
63 X,Z=H; Y=NO ₂	1.65±0.17
64 X=H; Y,Z=OCH ₃	10.7±3.79
65 X,Y,Z=H	9.57±3.60
66 X,Y=H; Z=Cl	11.4±6.79
67 X=H; Y,Z=CH ₃	43.5±18.5

IC₅₀ values were determined spectrophotometrically with kynuramine as substrate.

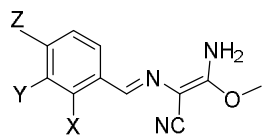
TABLE 5 IC₅₀ values (μM) for inhibition human MAO A by 4-aryloxy-3,5-diamino-1*H*-pyrazoles **68-72**.



	X, Y, Z	hMAO A IC ₅₀ (μM)
68	X,Y,Z=H	>100
69	X,Y=H; Z=Cl	19.7±17.9
70	X,Z=H; Y=NO ₂	420±250
71	X=H; Y,Z=OCH ₃	>100
72	X=H; Y,Z=CH ₃	>100

IC₅₀ values were determined spectrophotometrically with kynuramine as substrate.

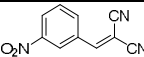
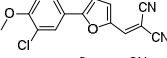
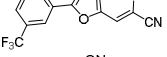
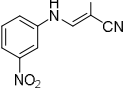
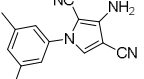
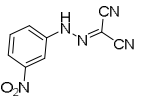
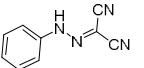
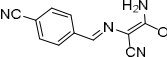
TABLE 6 IC₅₀ values (μM) for inhibition of human MAO A by (*E,E*)-4-amino-1-aryl-3-cyano-4-methoxy-2-azabutadienes **73-75**.



X, Y, Z	hMAO A IC ₅₀ (μM)
73 X,Y,Z=H	251±95.1
74 X,Y=H; Z=OCH ₂ CHCH ₂	113±130
75 X,Y=H; Z=CN	1.92±0.927

IC₅₀ values were determined spectrophotometrically with kynuramine as substrate.

Table 7 IC₅₀ values (μM) for inhibition of human MAO A, MAO B and AChE by selected compounds (25, 31, 32, 49, 60, 63, 65, 75).

Comp.	Structure	IC ₅₀ (μM) after 5 min preincubation		
		hMAO A	hMAO B	hAChE
25		44.7±20.6	24.6±9.4	
31		0.34±0.05	0.26±0.11	52±8
32		0.12±0.03	15.2±5.3	48±2
49		>100	21.5±2.5	
60		(>100)	(>100)	
63		12.2±4.1	3.80±0.31	44±5
65		22.9±1.5	<10% at 25 μM	<10% at 100 μM
75		3.41±0.83	3.45±0.52	71±10
ASS234 [†]		0.053±0.004*	1.2±0.1 [‡]	0.23±0.02

IC₅₀ values were determined in the coupled assay with tyramine (2xK_M).

[†] Bolea et al., 2011.

[‡] Without preincubation (i.e., reversible binding)

Table 8 IC₅₀ values and binding energies E_{bin} towards

hMAO A for **25**, **30**, **49**, **63**, **65**, and harmine.

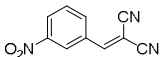
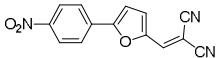
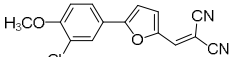
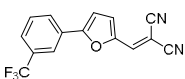
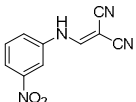
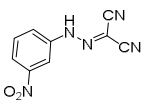
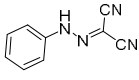
Comp.	Structure	MAO A IC50 (μM)	E _{bin} (kJ/mol)
25		9.05 \pm 0.091	321.6
30		15.7 \pm 1.87	338.3
31		0.34 \pm 0.05	368.2
32		0.12 \pm 0.03	377.6
49		9.65 \pm 1.36	323.6
63		1.65 \pm 0.17	346.7
65		9.57 \pm 3.60	272.7
Harmine		5-17 nM	395.6

Figure Legends

SCHEME 1 General procedure for the Knoevenagel condensation reaction regarding the syntheses of arylidenepropanedinitriles of type **3** (compounds **16-41**, Table 1) and the new compounds **31**, **34**, **35** and **36**.

SCHEME 2 General procedure for the syntheses of [(phenylamino)methylidene]propanedinitriles of type **6** (compounds **42-52**, Table 2) and the new compounds **45**, **48** and **52**.

SCHEME 3 General procedure for the syntheses of both 4-amino-1-phenyl-1*H*-pyrrole-3-carbonitriles and 3-amino-1-phenyl-1*H*-pyrrole-2,4-dicarbonitriles of type **8** (compounds **53-62**, Table 3) and the new compounds **59**, **60**.

SCHEME 4 General procedure for the syntheses of (phenylhydrazinylidene)propanedinitriles of type **11** (compounds **63-67**, Table 4) and the new compound **67**.

SCHEME 5 General procedure for the syntheses of 4-arylazo-3,5-diamino-1*H*-pyrazoles of type **12** (compounds **68-72**, Table 5) and the new compound **72**.

SCHEME 6 General procedure for the syntheses of (*E,E*)-4-amino-1-aryl-3-cyano-4-methoxy-2-azabutadienes of type **15** (compounds **73-75**, Table 6) and the new compounds **74** and **75**.

FIGURE 1. The structures of all the new arylidenepropanedinitriles (**31**, **34**, **35**, **36**), the [(phenylamino)methylidene]propanedinitriles (**45**, **48**, **52**), the 3-amino-1-phenyl-1*H*-pyrrole-2,4-dicarbonitriles (**59**, **60**), the (phenylhydrazinylidene)propanedinitrile **67**, the 4-arylazo-3,5-diamino-1*H*-pyrazole **72**, and the (*E,E*)-4-amino-1-aryl-3-cyano-4-methoxy-2-azabutadienes **74** and **75**.

FIGURE 2 Potential disaggregating effect of **31**, **32**, **33** and **37** on A β_{1-42} fibrils. Different concentrations (20, 40 and 60 μ M) of compounds were added to A β_{1-42} samples (pre-incubated at 37°C for 24 h) and incubated at 37°C for an extra 24 h. The levels of fibrils were evaluated by the intensity of fluorescence of ThT. The fluorescence of fibrillary A β_{1-42} (fib), which was incubated at 37°C for a total time of 48 h, was also measured; and the fluorescence of other experimental conditions were indicated as arbitrary units (a.u.) related to A β_{1-42} . The fluorescence of A β_{1-42} fresh solution (N-fib) was also measured as reference. Data are mean \pm SEM of 3-4 independent experiments.

FIGURE 3 Potential disaggregating effect of **63**, **65** and **75** on A β_{1-42} fibrils. Different concentrations (20, 40 and 60 μ M) of compound were added to A β_{1-42} samples (pre-incubated at 37°C for 24 h) and for another 24 h incubation period at 37°C. The levels of fibrils were evaluated by the intensity of fluorescence of ThT. The fluorescence of fibrillary A β_{1-42} (fib), which was incubated at 37°C for a total time of 48 h, was also measured; and the fluorescence of other experimental conditions were indicated as arbitrary units related to A β_{1-42} . The fluorescence of A β_{1-42} fresh solution (N-fib) and of A β_{1-42} incubated with resveratrol (20 μ M res), a known anti-aggregating compound, were also measured as reference. Data are mean \pm SEM of 3-4 independent experiments. $p < 0.05$ statistical different from A β_{1-42} fib.

FIGURE 4 Most probable tautomers of compounds **49**, **63** and **65**.

FIGURE 5 Comparison of the location of **49** (magenta), **63** (element color) and **65** (green) in the proximity of FAD.

FIGURE 6 Charge distribution of compound **63**.

FIGURE 7 Charge distribution of compound **49**.

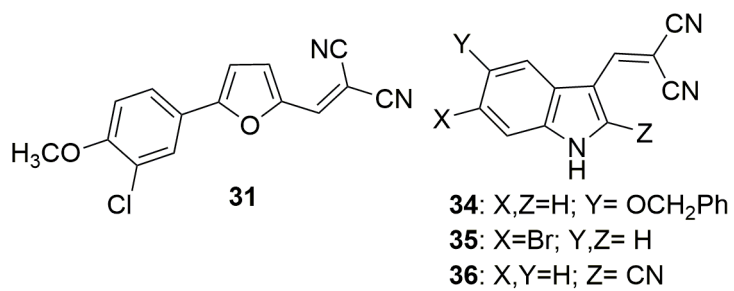
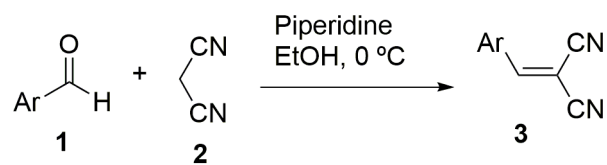
FIGURE 8 Interactions of **31** and **32** with MAO A.

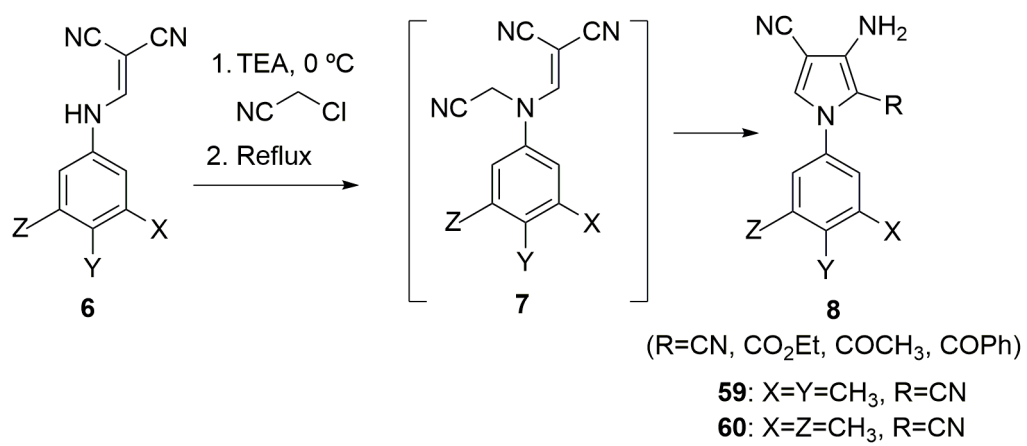
FIGURE 9 Interactions of **31** and **32** with MAO B.

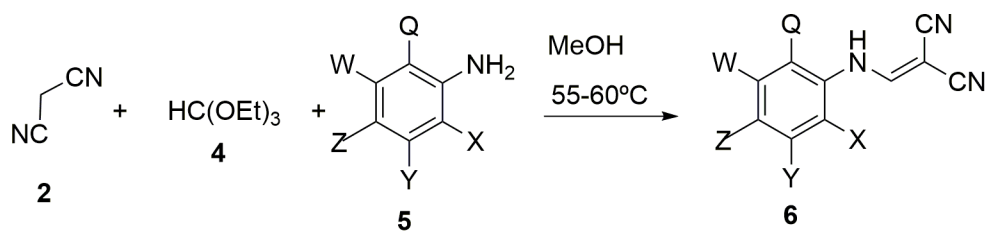
FIGURE 10 Binding mode of **82** and **83** at the active site of hAChE.

FIGURE 11 Overall view of **82** (blue, up) and **83** (down) immersed in hAChE protein (4M0F PDB model) viewed through the gorge of the protein surface. Red circles represent water molecules.

FIGURE 12 Lipophilic potential on the surface of **83**. Blue – hydrophilic values, yellow – hydrophobic.



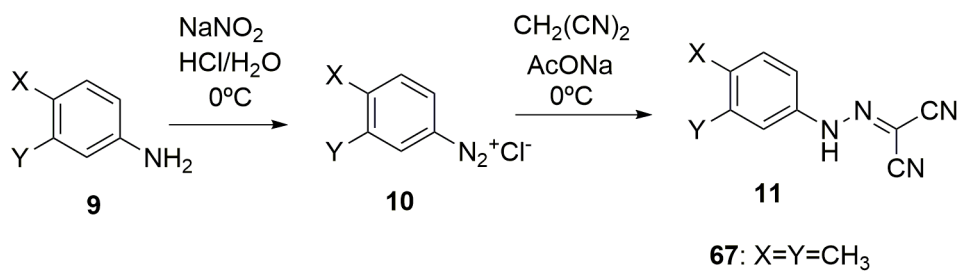


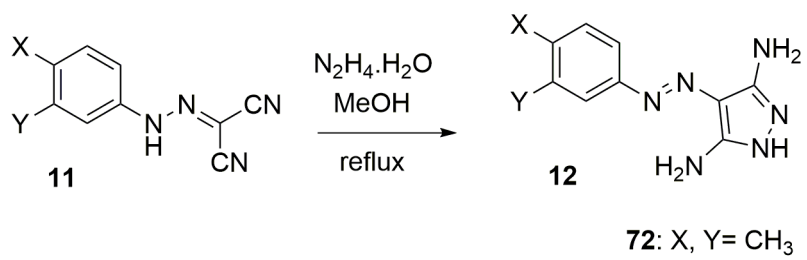


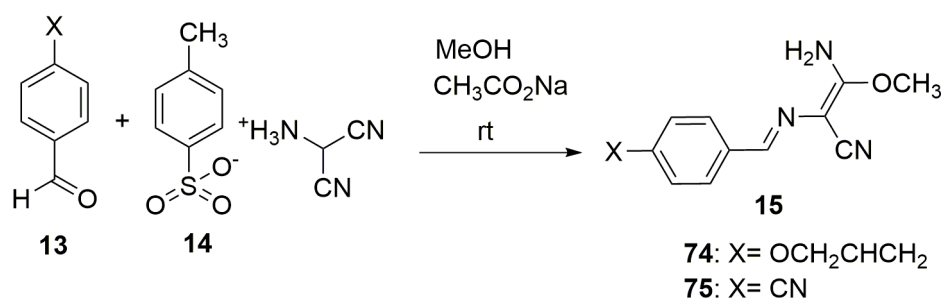
45: X,Z,Q= CH₃; Y,W= H

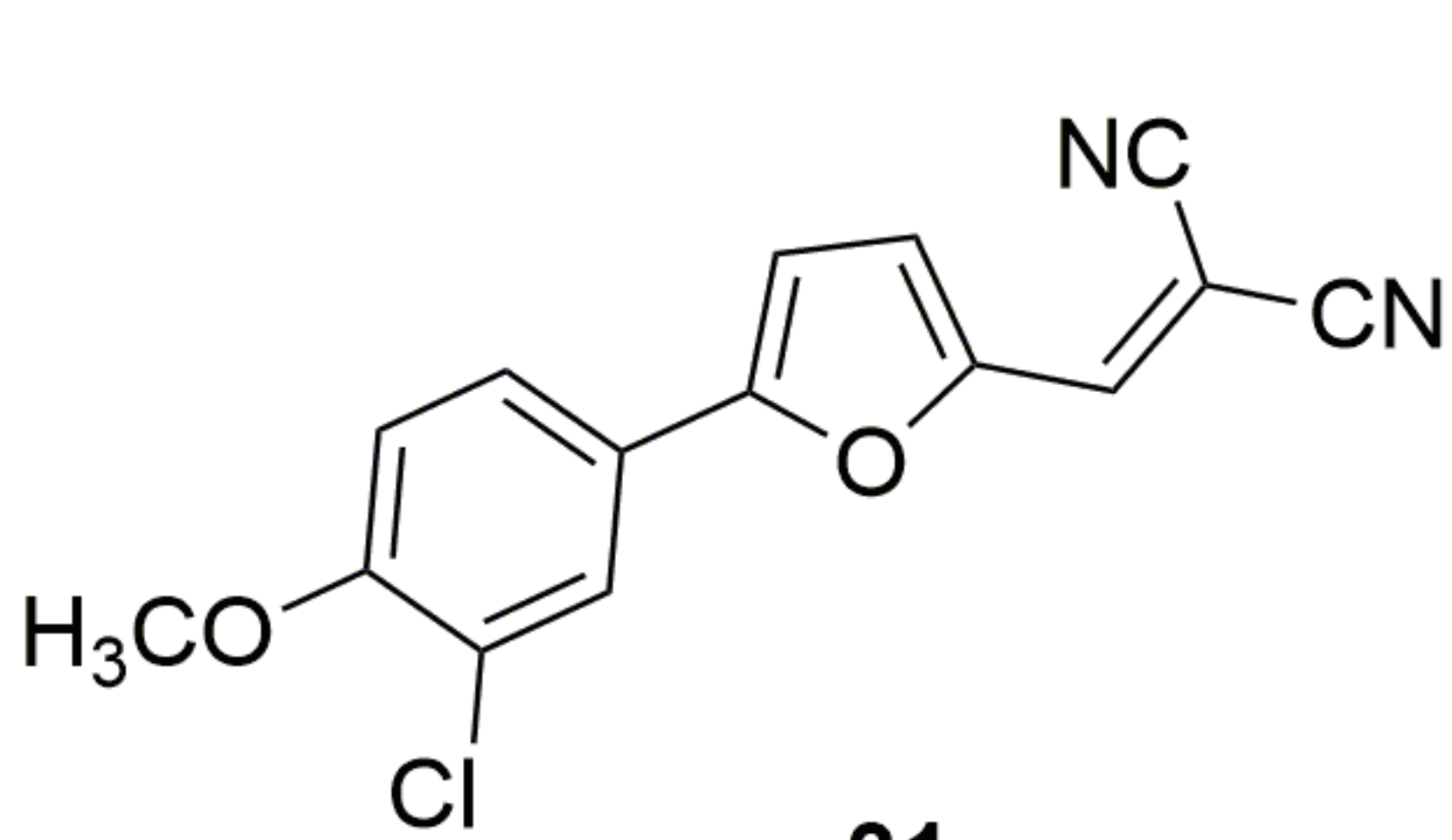
48: X,W,Q= H; Y,Z= OCH₃

52: X,Q= CH₃; Y,W= H; Z= Br

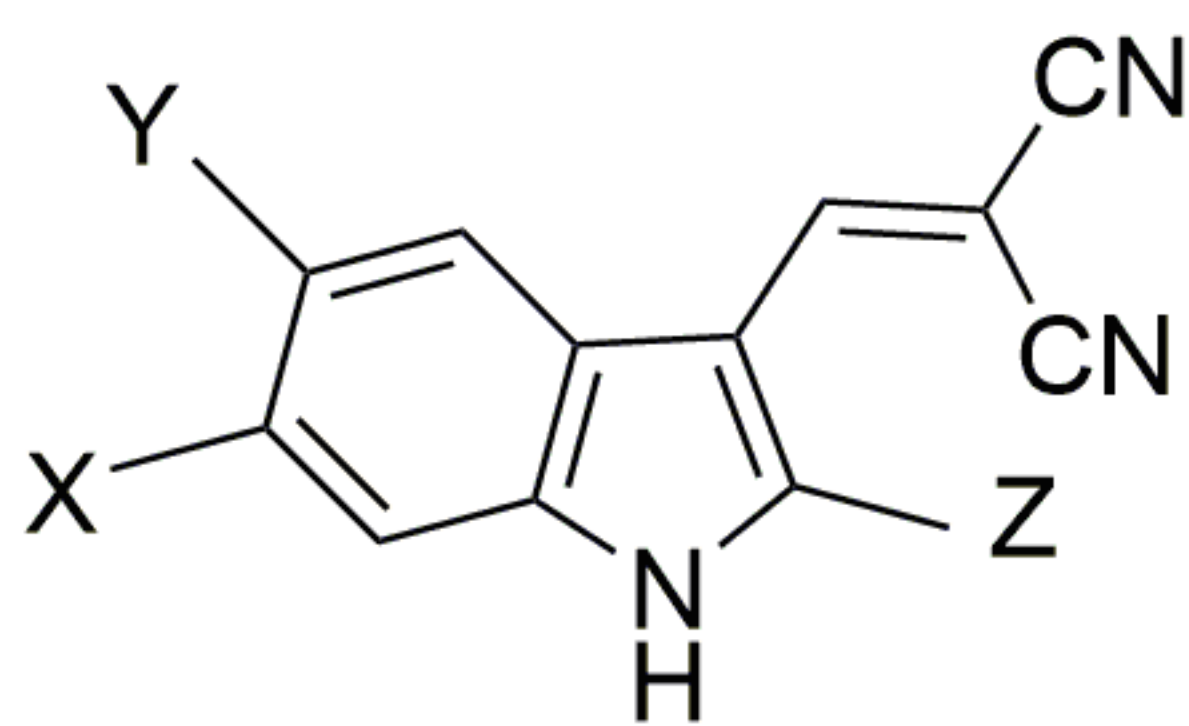








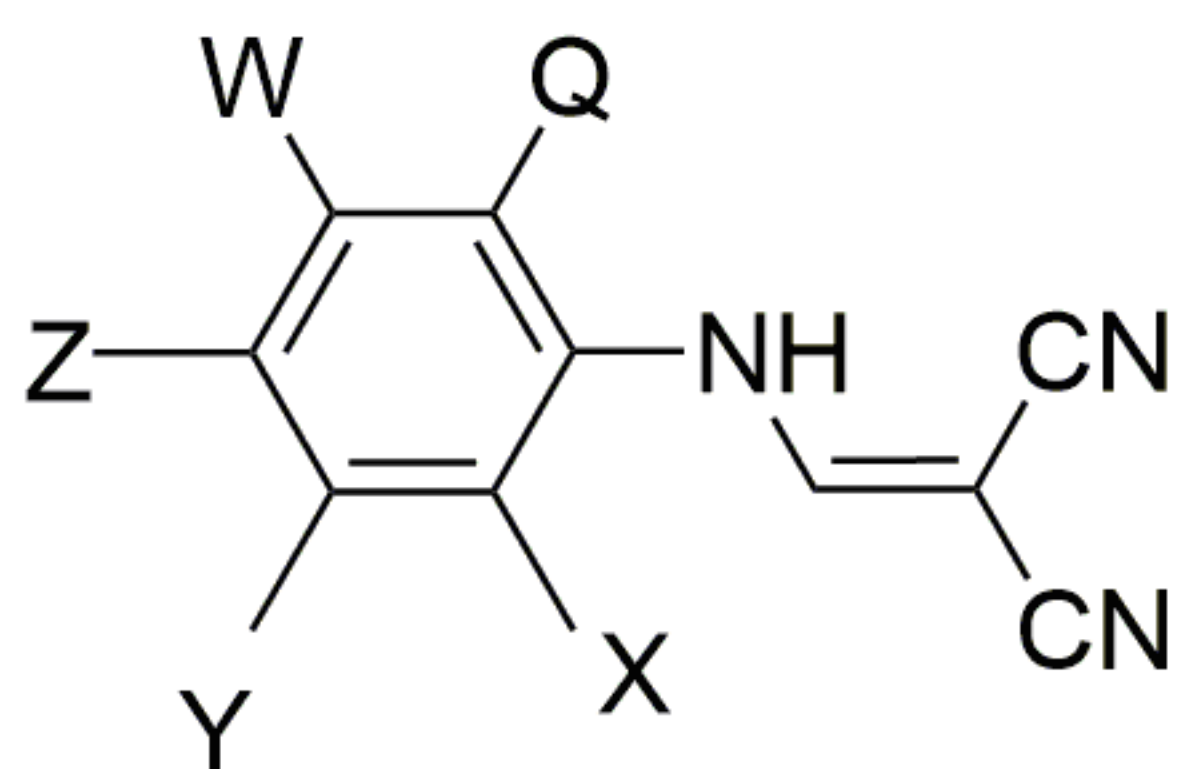
31



34: X,Z=H; Y=OCH₂Ph

35: X=Br; Y,Z=H

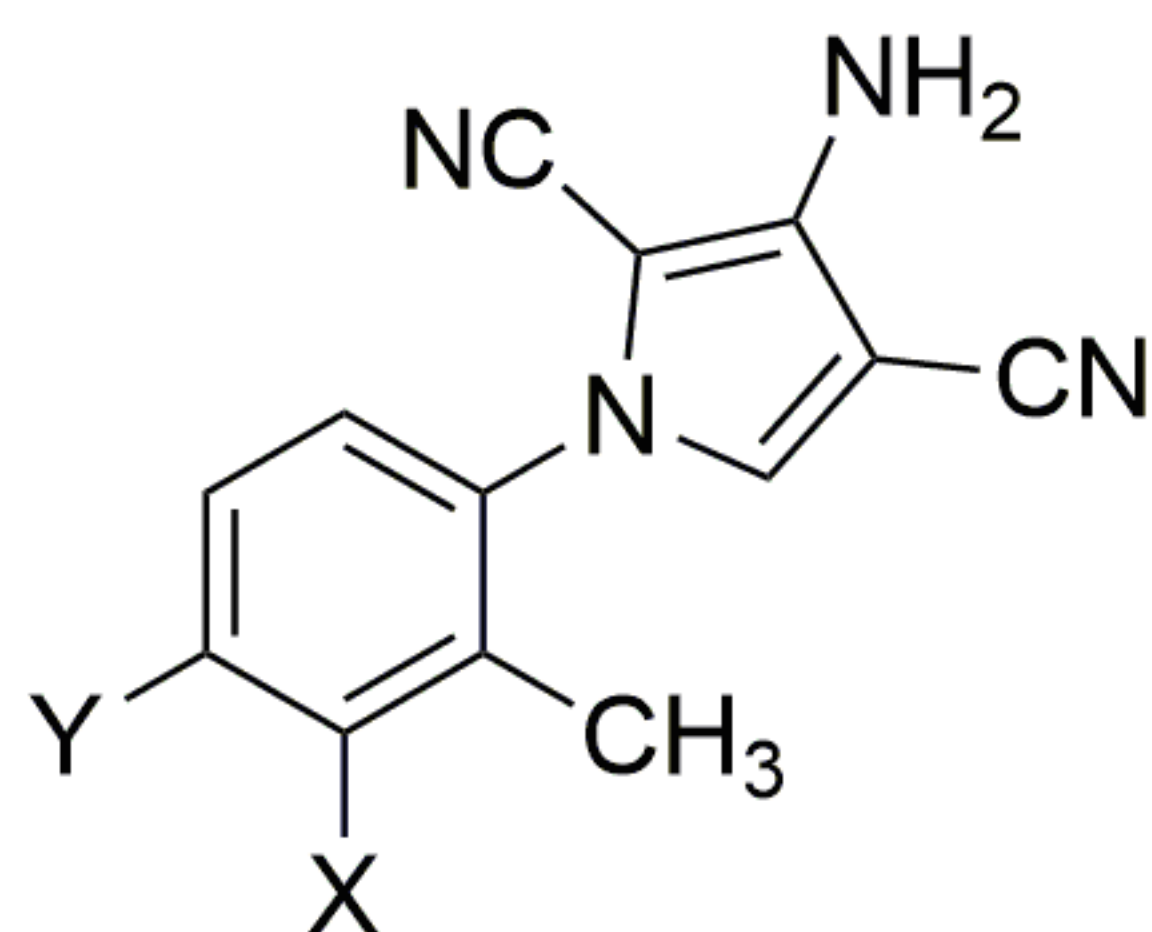
36: X,Y=H; Z=CN



45: X,Z,Q= CH₃; Y,W=H

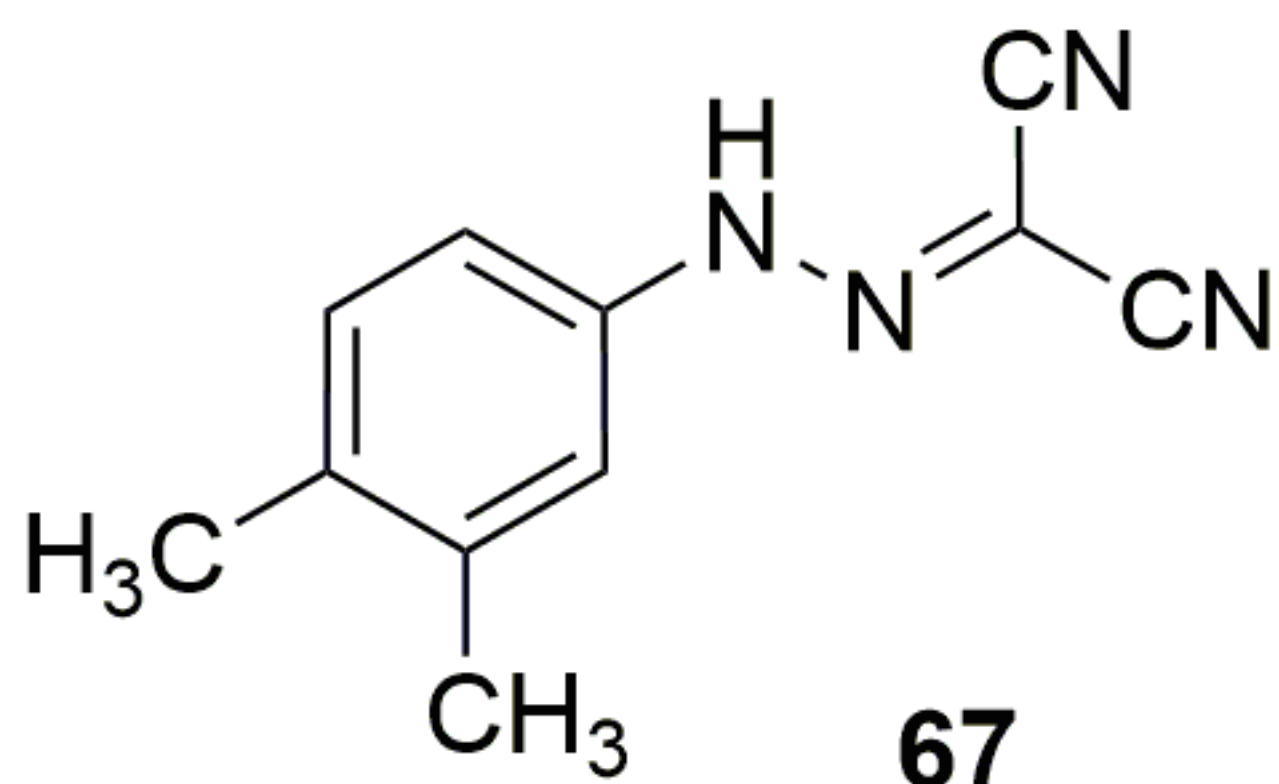
48: X,W,Q=H; Y,Z=OCH₃

52: X,Q=CH₃; Y,W=H; Z=Br

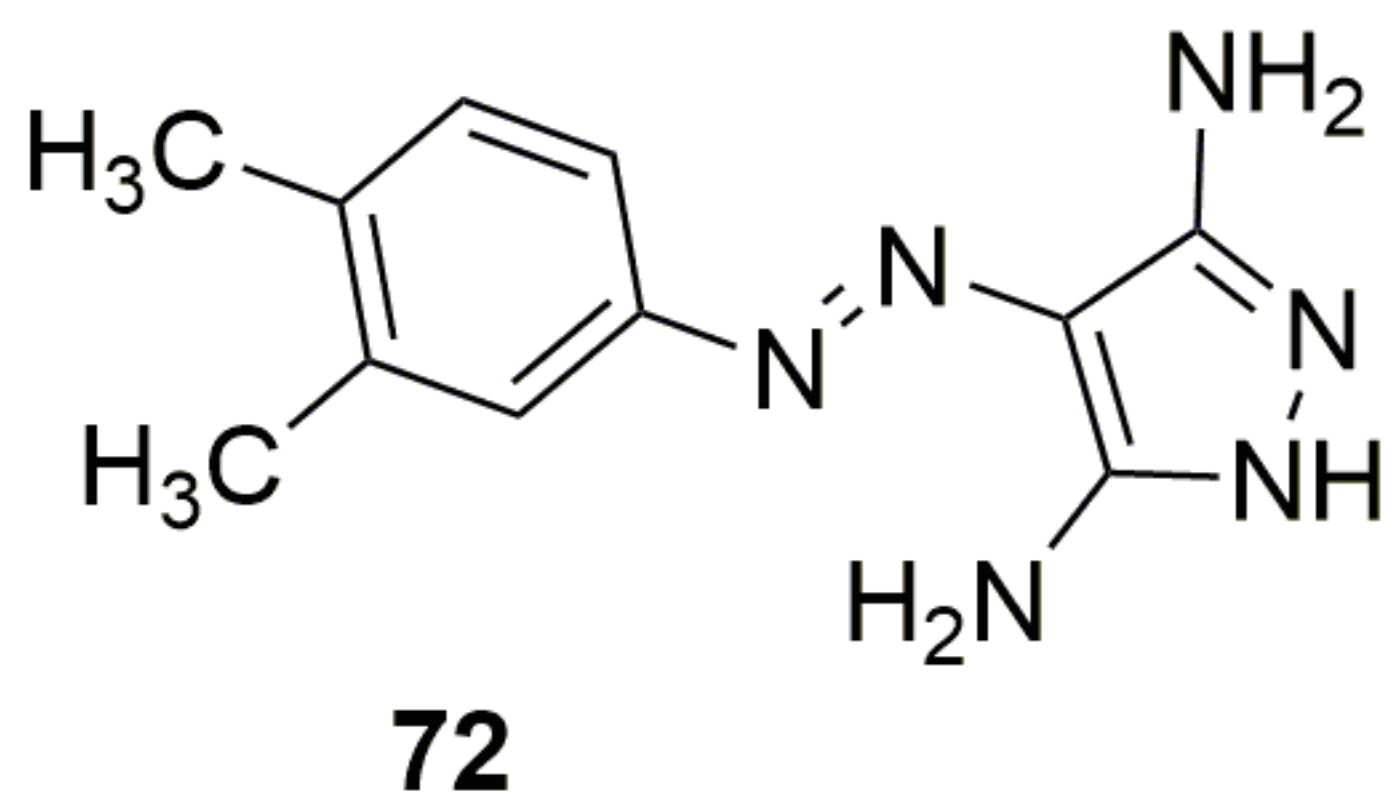


59; X=CH₃; Y=H

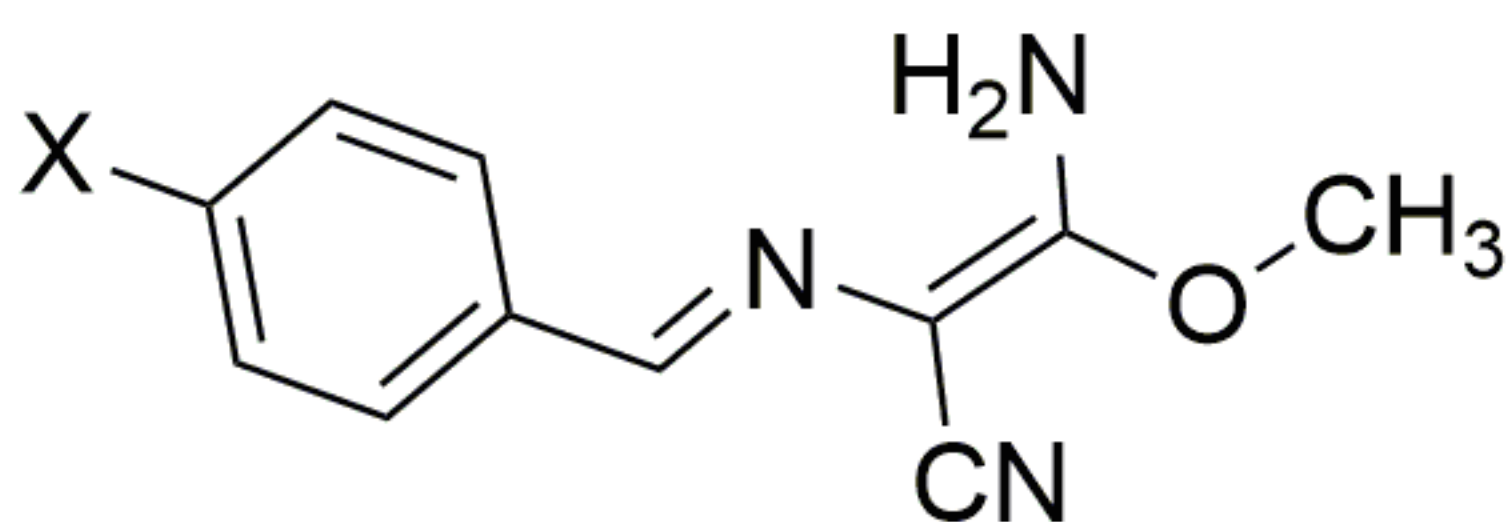
60:X=H; Y=CH₃



67



72



74: X= OCH₂CHCH₂

75: X= CN

